ELSEVIER

Nanostructural metallic materials: Structures and mechanical properties

L.G. Sun [1,2,†], G. Wu [1,3,†], Q. Wang [1,4,†], J. Lu [1,5,6,*]

[1] Department of Mechanical Engineering, City University of Hong Kong, Hong Kong, China
[2] School of Science, Harbin Institute of Technology, Shenzhen 518055, China
[3] Max-Planck-Institut für Eisenforschung, Max-Planck-Straße 1, 40237 Düsseldorf, Germany
[4] Laboratory for Microstructures, Institute of Materials, Shanghai University, Shanghai 200072, China
[5] Hong Kong Branch of National Precious Metals Material Engineering Research Center (NPMM), City University of Hong Kong, Hong Kong, China
[6] Center for Advanced Structural Materials, City University of Hong Kong Shenzhen Research Institute, Greater Bay Joint Division, Shenyang National Laboratory for Materials Science, Shenzhen, China

The trade-off of strength and ductility of metals has long plagued materials scientists. To resolve this issue, great efforts have been devoted over the past decades to developing a variety of technological pathways for effectively tailoring the microstructure of metallic materials. Here, we review the recent advanced nanostructure design strategies for purposely fabricating heterogeneous nanostructures in crystalline and non-crystalline metallic materials. Several representative structural approaches are introduced, including (1) hierarchical nanotwinned (HNT) structures, extreme grain refinement and dislocation architectures etc. for crystalline metals; (2) nanoglass structure for non-crystalline alloys, i.e. metallic glasses (MGs); and (3) a series of supra-nano-dual-phase (SNDP) nanostructures for composite alloys. The mechanical properties are further optimized by manipulating these nanostructures, especially coupling multiple advanced nanostructures into one material. Particularly, the newly developed SNDP nanostructures greatly enrich the nanostructure design strategies by utilizing supra-nano sized crystals and MGs, which exhibit unique size and synergistic effects. The origins of these gratifying properties are discussed in this review. Furthermore, based on a comprehensive understanding of microscopic mechanisms, a broad vision of strategies towards high strength and high ductility are proposed to promote future innovations.

Introduction

Crystalline materials with nanotwinned (NT) structures have been studied for several decades. It is well known that NT structures are beneficial for the improvement of strength and plasticity of metallic materials [1,2] and strengthening superhard materials such as boron nitride and diamond [3–5]. The mechanical behaviors and properties of NT materials can be optimized by tailoring NT structures and exhibit significant anisotropy [6–11]. In the past years, many researchers observed a kind of NT architecture obtained by virtue of advanced processing techniques such as equal channel angular pressing (ECAP) [12]. Such architecture is called hierarchical nanotwinned (HNT) structure. The materials with HNT structures exhibit attractive mechanical and physical properties [13,14]. Pioneering theoretical and molecular dynamics (MD) studies have been conducted on HNT structures [15–18]. Afterwards, the experimental efforts identified that HNT structures have potential to break down the strength-ductility trade-off of materials [19,20]. Hence, introducing HNT structures into materials is becoming a charming topic. It is found that HNT structures are most commonly engineered in the steels [21–24], medium or high entropy alloys (MEAs or HEAs) [25–28]. Recently, a scale law for hierarchical

* Corresponding author.
E-mail address: Lu, J. (jianlu@cityu.edu.hk)
† These authors contributed equally to this work.

 https://doi.org/10.1016/j.mattod.2020.04.005

twinning is derived in stainless steels [29]. In addition, the high-order HNT structures are produced in silver [30]. The twin spacing dependent high-order hierarchical twinning mechanisms are studied by MD simulations [31]. Mechanism-based plasticity modeling verifies high strength and high ductility of HNT structures [32]. HNT structure is also drew attention in the recent review articles as a kind of heterogeneous nanostructure [33,34].

By virtue of advanced surface processing techniques such as surface mechanical grinding treatment (SMGT) [35], another promising approach is reported to be associated with gradient grain size for metals. It has been clarified that the gradation of grain size induces stress/strain gradient, promoting strain hardening and delaying strain localization during plastic deformation [36–38] and thus, attaining extraordinary mechanical properties. In addition, the gradient structure can also be combined with other strengthening mechanisms such as transformation-induced plasticity (TRIP) effect [22] and NT structures [19,20].

For the nanocrystalline materials, strengthening transfers to softening with grain refinement due to the inverse Hall–Petch effect, which is generally attributed to the unstable grain boundaries (GBs) of extremely fine grains. To stabilize GBs, many microstructural processes are developed such as GB relaxation [39], texturing [40,41] and solute segregation [42]. The low-angle GBs are as effective in hindering dislocation motion as high-angle GBs [41,43]. Segregation of impurities into GBs reduces their interface energy [44]. The relaxation and impurity segregation to the GBs can help to stabilize the GBs and break down the limit of the critical grain size for inverse Hall–Petch effect. By GB relaxation, a great increase of hardness is achieved for extremely fine-grained nanostructure [45].

Dislocation is another kind of crystalline defect that scientists can play with to design high-performance crystalline materials. According to the well-known Taylor hardening law [46], the strength increases with dislocation density. Pursuing high dislocation density is still an effective way to improve the strength of materials [47,48]. Besides, researchers are also dedicated to improving the ductility of materials via the control of dislocations. For instance, good ductility is accessible through dynamic recovery of dislocations through heat treatment [49,50]. The addition of hydrogen into metals influences the dislocation activity and plastic behavior [51,52]. Solid solutes are able to diffuse into dislocations [53,54] or act as the aggregation positions for dislocations [55]. Furthermore, dislocations can form tangled dislocation structures, exhibiting higher stability than random dislocations [56]. These dislocation structures show various heterogeneous configurations such as dislocation channels [57,58], dislocation cells and walls [59–61] and lath structures [62]. High density of dislocations renders the interfaces immobile [63] while the interaction between dislocations and solid solutes may accelerate the transformation process [64]. Strain partitioning is also partly ascribed to the effect of dislocations [65]. Recently, a new steel with high strength and high ductility is produced [66]. The high dislocation density accounts for the excellent mechanical properties by the synergy of dislocation forest hardening, propagation of mobile dislocations and controllable TRIP effect. Therefore, the mechanical properties of materials can be optimized via the manipulation of dislocation density and morphologies.

It has been widely recognized that the improvement of structural and/or functional properties of crystalline materials can be realized via modifying their chemical structure (e.g. introducing different phase or varying their composition, etc.) and/or structural defects (such as dislocations or GBs) [67]. Nevertheless, it is not easy to be adapted for the metallic glasses (MGs) due to their disordered atomic structure without a long-range translational symmetry. Since their discovery in the 1960s, MGs have long been known as a promising advanced structural material because of their excellent mechanical properties [68]. However, in stark contrast to their crystalline counterparts, MGs suffer from inhomogeneous plastic deformation mode associated with highly localized plastic deformation into shear bands at room-temperature and usually exhibit poor ductility in unconstrained loading geometries [69]. Therefore, the practical structural application of MGs is extremely impeded. To achieve the room-temperature ductility, particularly in tension, large efforts have been devoted to finding an effective way to initiate and multiply shear bands for macroscopic plastic deformation [70]. Up to now, apart from the introduction of nano- (or supra-nano-) secondary crystalline phases into MGs, the formation of amorphous nanostructure is considered as another effective way to develop advanced metallic materials [67,71–76]. According to Gleiter [73], the nanostructured MGs, with a characteristic of nanometer sized glassy regions interconnected by glass/glass interfaces, are supposed to be a new non-crystalline structure. The purposely designing of nanostructure for MGs could allow for the tailoring of their chemical and/or structural properties. Over the past two decades, several different technical approaches have been proposed for synthesizing nanostructured MGs, including inert gas condensation, magnetron sputtering, pulsed electrodeposition, and severe plastic deformation etc. [74]. Compared to their bulk glass counterparts, these nanoglass MGs (NGMGs) exhibit unusual mechanical [77–80], magnetic [81] and biomedical [82,83] properties.

Researchers hope to utilize the advantages of both crystalline and amorphous materials simultaneously by fabricating a composite system. Recently, a new class of nanostructured materials has been successfully fabricated by a combination of both crystalline and amorphous phases. The most impressive achievement is that, a magnesium alloy with the structure of supra-nano-dual-phase glass-crystal (SNDP-GC) was invented by Ge Wu, Jian Lu, et. al. [71], where 'supra-nano' is defined as the size with a range of 1–10 nm. The structural units with the size in this range are called supra-nanostructure. This term is used to divide a new range of length scale which is different from 'sub-nano' and 'nano'. Because many nanostructural metallic materials composed of structural units within supra-nano dimension display totally different mechanical properties and deformation mechanisms compared with that comprised of nano-sized structural units, 'supra-nano' is adopted to describe this family of new metallic materials. As a representative, the SNDP-GC magnesium alloy possesses an ultrahigh strength that lies in the near-ideal regime $E/20$, where E is the Young's modulus of a material. In materials science, it is very difficult to fabricate the near-ideal strength materials, which usually possess 'perfect' crystalline structures. The conventional near-ideal strength materials are usually single crystalline whiskers [84], crystalline nanowires

[85] or nano-sized MGs [86], which contain very few defects. It is obvious that the complicated fabrication condition and the nano-sized feature of the 'perfect' structural materials limit their applications. It is very challenging to fabricate near-ideal strength materials with large size, against the 'smaller is stronger' rule in materials. With the increase of material size, the enrichment of structural defects such as dislocation and free volume contributes to the softening of crystalline and amorphous materials, respectively. How about scaling down structural units but maintain the size of the whole materials? However, several kinds of materials with single phase supra-nano units [87,88] become softer instead (although other interesting properties occur, such as large plasticity), as a result of soft nature of the interface between the units. SNDP nanostructuring resolved the dilemma. The two phases include supra-nano-sized crystalline phase and amorphous phase. The unit size of each phase is extremely small, which contains few defects. The SNDP-GC structure builds up a large sized magnesium alloy with the dimension of 100 mm × 100 mm × 10 μm, which achieved a near-ideal strength of 3.3 GPa. More recently, a detailed structural study of Mg-based SNDP material is conducted which is synthesized by annealing of Mg-based MGs [89].

In the following sections, a brief review will be given for the progresses in research on crystalline, amorphous and SNDP materials, particularly concentrating on the microstructure and mechanical properties. Note that some of other popular strategies for high-strength and high-ductility structural materials design, such as nanoprecipitation [90,91] and phase transformation [25,66] can also be combined with the above mentioned advanced structures. Some nanostructures for crystalline/non-crystalline/composite metallic materials reviewed in this paper are presented in Fig. 1. In addition, as a rapidly developing advanced material and structure processing technology, additive manufacturing (AM) is now widely used for the synthesis of nanostructural metallic materials. The researchers are devoted to tailoring the microstructures and mechanical properties, which are dependent on process parameters, alloy composition, layer thickness and part geometry etc. [92–95]. On the other hand, machine learning has been gradually employed to predict and design high-performance materials [96]. However, the development of microstructure-based predictive modeling for machine learning is still in its infancy and only GBs are paid attention so far [97,98]. A brief introduction for these topics is also given in this review.

Hierarchical nanotwinned structures

Nanotwinned (NT) structures can efficiently block the motion of dislocations, promoting strain hardening for the enhancement of materials. Indeed, the hierarchical nanotwinned (HNT) structures can also serve as dislocation barriers. The NT structures with single orientation may only hinder dislocations in limited directions while the HNT structures construct a complicated three-dimensional architecture, which could be more effective in impeding dislocations. Hence, such hierarchical nanostructure may have great significance for high-performance materials design.

Spatial distribution of HNT structures

The spatial distribution of HNT structures depends on the location of twin planes. In face-centered cubic (FCC) metals, the dihedral angle between two orders of hierarchical twins is about 70° [30]. It means that the two-dimensional distribution of HNT structures could be as Fig. 2a. In fact, such distribution is only a special case that all the twin planes are perpendicular to a same reference plane (Fig. 2b). From a three-dimensional perspective, there exist more abundant HNT architectures. As shown in Fig. 2c, the original tetrahedron (gray), which represents the twinning system in FCC metals, can derive twin planes along every other tetrahedrons (red). Similarly, the derived tetrahedrons (red) can form more twin planes through the combination with more tetrahedrons (blue and green). The planes between every two adjacent tetrahedrons represent the spatial orientations of twin planes. Note that all these twin planes intersect with each other. From this point of view, the fabrication of HNT structures can three-dimensionally impede the propagation of dislocations for strengthening and act as dislocation nucleation sites to improve ductility.

Metals with HNT structures

Many studies reported that steels with a combination of heterogeneous nanostructures can simultaneously achieve high strength and high ductility, in which the HNT structures should play an important role. The 304 stainless steels prepared by surface mechanical attrition treatment (SMAT) can combine the benefit of transformation-induced plasticity (TRIP) effect and nanostructures (such as NT/HNT, gradient grain distribution and high dislocation density), achieving high strength and high ductility [22]. Note that HNT-based rhombic blocks can be fabricated in SMATed steels (Fig. 3a). The twinning-induced plasticity (TWIP) steels obtained from cold rolling and heat treatment also exhibit excellent mechanical properties. The high yield strength (YS) and ultimate tensile strength (UTS) with good ductility (~1.45 GPa, ~1.6 GPa and ~25%, respectively) may originate from the formation of HNT structures during tensile deformation [21]. The TWIP steels with gradient HNT structures (Fig. 3b) obtained from pre-torsion and subsequent tensile deformation, exhibiting better performance of working-hardening and evading the strength-ductility trade-off dilemma [20,24]. The higher order HNT structures are observed in SMATed TWIP steels during tensile testing [19], exhibiting an ultrahigh YS of ~2 GPa while still retaining a considerable uniform elongation of ~15%. Austenitic 316L stainless steels additively manufactured via a laser powder-bed-fusion technique exhibit a high YS and good tensile ductility [23]. The well-aligned HNT structures are observed inside a grain (Fig. 3c).

On the other hand, CrCoNi medium entropy alloys (MEAs) show better mechanical properties than high-entropy CrMnFeCoNi, mainly owing to their low stacking fault energy (SFE) for easier twinning [26]. The YS, UTS and ductility increase from 265 ± 10 MPa to 360 ± 10 MPa, 600 ± 40 MPa to ~870 MPa and ~30% to ~38% respectively. The study on Mo alloyed FeCoCrNi high entropy alloys (HEAs) (with a low SFE of ~19 mJ/m^2) demonstrated that solute strengthening and twin/microband induced plasticity can improve the mechanical properties of HEAs with superb ductility of ~51%, YS of ~328 MPa and UTS

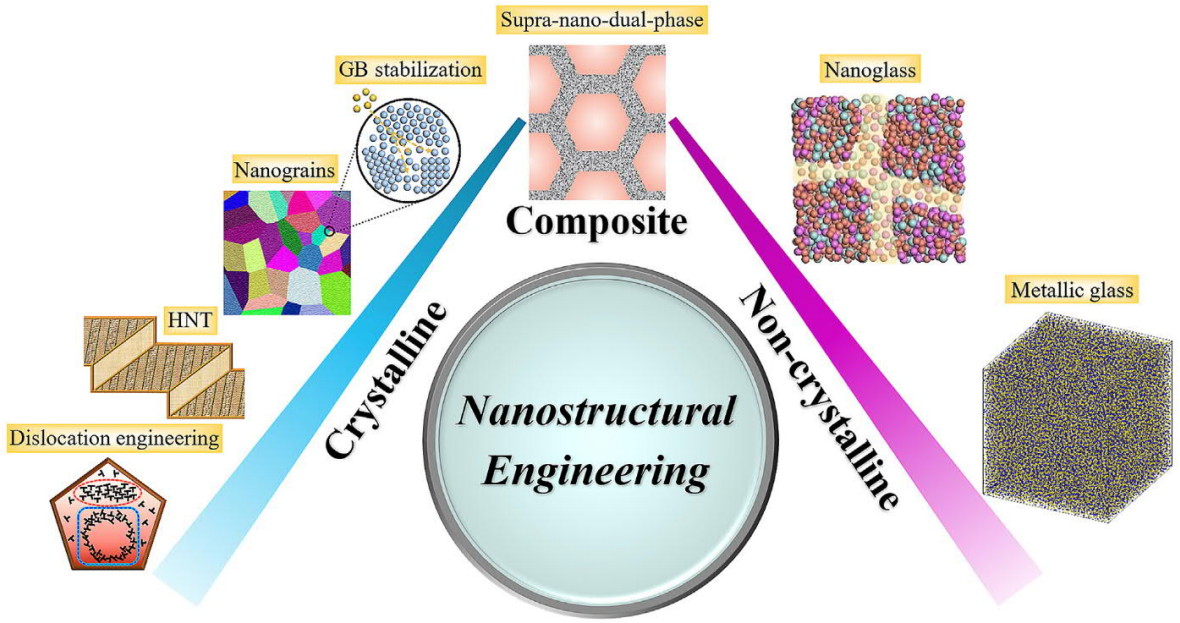

FIGURE 1

A schematic illustration of some nanostructures tailored in crystalline/non-crystalline/composite metallic materials for high strength and high ductility.

of ~784 MPa [28]. HNT structures should be beneficial for the blockage of dislocations multi-directionally (Fig. 3d). Note that the SFE in steels, MEAs and HEAs is tunable and even reach the negative SFE at cryogenic temperatures and thus, HNT structures are gradually becoming achievable in materials with low SFE.

However, the question of how the HNT structures solely strengthen metals is still ambiguous because all the metals mentioned above mix hierarchical nanostructures. In order to further reveal the deformation mechanisms and strengthening effect of HNT structures, it is essential to develop pure metals with HNT structures. Recently, the high-order HNT structures have been successfully fabricated in pure Ag (Fig. 3e) [30]. High-order HNT structures can further improve the mechanical properties of Ag via effective interplay between HNT structures and dislocations (Fig. 3f). In particular, the YS and ductility of high-order HNT Ag (~145 MPa and ~35%) is better than low-order HNT Ag (~125 MPa and ~24%).

Besides, theoretical studies have predicted some interesting phenomena. By virtue of a dislocation-based theoretical model, Zhu et al. unveiled the effect of twin thicknesses of primary and secondary twin lamellae on the YS of metals [15]. It is found that there exists an optimal combination of twin thicknesses to achieve maximum strength, which is verified by MD simulations [17,18]. The different deformation mechanisms are observed with the variation of primary and secondary twin thicknesses, explaining the corresponding strengthening and softening mechanisms. Furthermore, the theoretical models developed by Zhu et al. predict the nucleation of subordinate twin lamellae with respect to the twin thickness of low-order twin lamellae [16], giving rise to a significant enhancement of strength. Hereafter, theoretical models are employed to quantitatively predict the crack nucleation [99], crack blunting [100] and fatigue crack growth behaviors [101] of HNT materials. In addition, the theoretical models for the quantitative prediction of size-dependent mechanical properties of high-order HNT materials have also been developed [16,32]. The theoretical studies unveiled that HNT structures give an additional enhancement of mechanical properties. These theoretical findings may provide insights to reinforce the mechanical properties of metals.

Tailoring the limit of grain size for strengthening

With the decrease of grain size, the strength of nanocrystalline metals always increases first (Hall–Petch relation) and decreases due to excessive grain refinement (inverse Hall–Petch effect). The critical grain size triggering this transition from strengthening to softening varies among different materials and most of them appears in the range of 10~30 nm. The transition is due to the change of deformation mechanisms: dislocation-dominated strain hardening vs. grain rotation and growth softening. Hence, the hysteresis or impedance of grain rotation and growth should be effective for the design of unprecedentedly strong metallic materials, in which the stability of grain boundaries (GBs) should be a key issue.

Stabilizing GBs

Nano-laminated structure with a large fraction of low-angle GBs shows great structural stability [41]. Because the low-angle GBs possess low-energy states which are helpful to nanostructure stabilization and structural refinement [102]. Note that the formation of low-angle GBs is tunable via altering strain rates and/or temperatures. On the other hand, the relaxation/heat treatment has been identified beneficial to stabilize GBs. For instance, the hardness of solid solution Ni–W nanocrystalline alloys can be

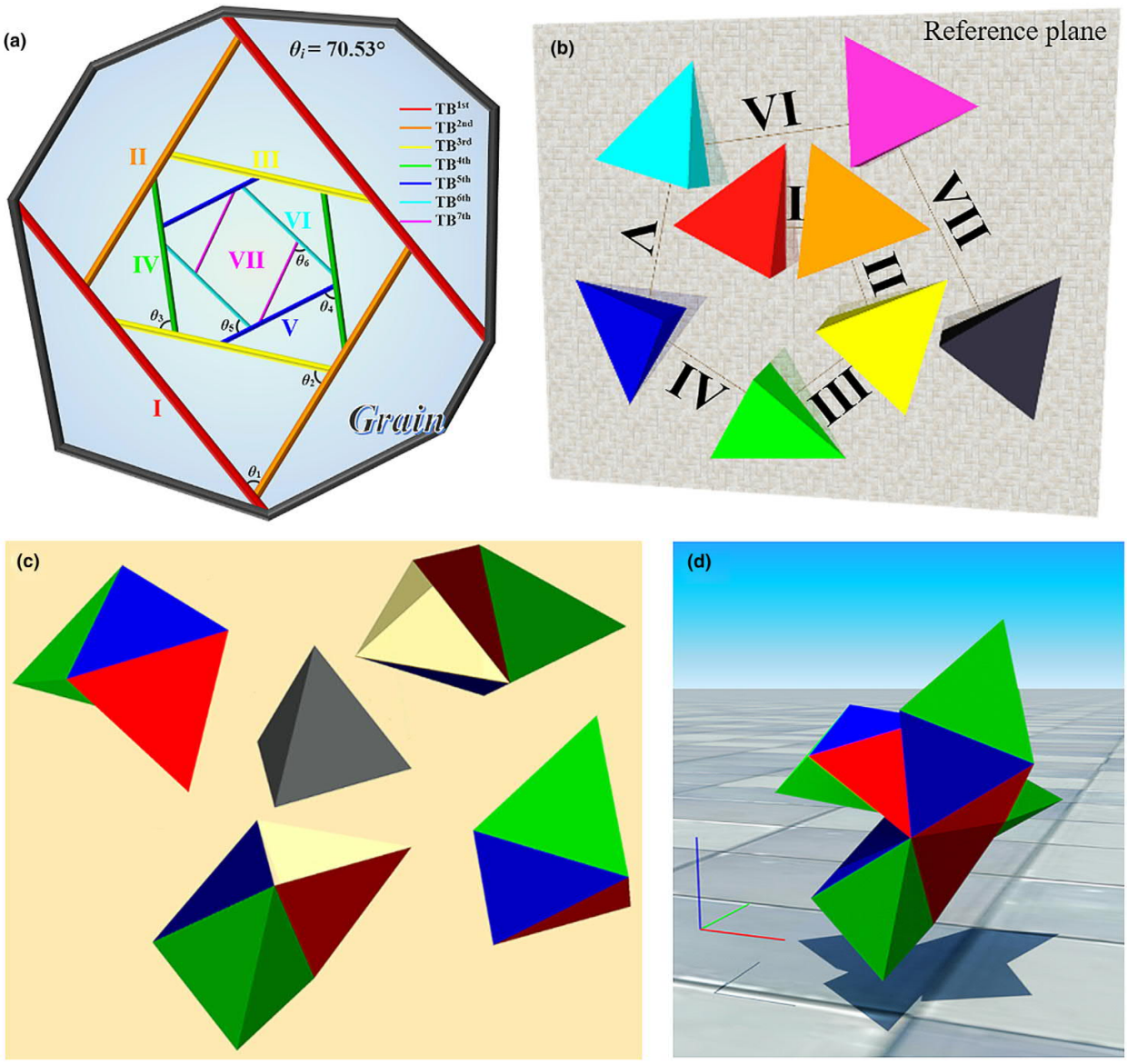

FIGURE 2

A diagram exhibiting the spatial distribution of twin planes. (a and b) The twin planes perpendicular to a same reference plane. (c and d) The three-dimensional stacking of tetrahedrons showing a three-dimensional distribution of twin planes.

improved with annealing, even for the finest grain size of ~3 nm [39]. Meanwhile, microalloying of Cu with Fe solute may induce the reduction of the boundary mobility and stabilize dislocations at GBs [103]. As shown in Fig. 4a, a glide dislocation is detected in Cu-Fe alloy with an extremely fine grain size. The limit of dislocation-based plasticity is extended to a smaller grain size of ~5 nm. Interestingly, the grain rotation induced softening most easily occurs with a grain size of ~70 nm in Ni [104] which is attributed to the interaction between the GB-mediated and grain interior-mediated dislocations. Generally speaking, small grain interior is more likely dislocation/defect-free. Thus, the metals with extremely fine grains may be dominated by the emission of dislocations from GBs during plastic deformation if grain rotation and growth are not induced, which may also avoid the grain rotation by the interaction between the dislocations inside the grains and from GBs.

On the other hand, the addition of nonmetallic impurities could be another choice for the stabilization of GBs. The recent comprehensive study by first principle simulations has compared the effect of H, B, C, N, O, Si, P and S elements on the energetics and mechanical strength of Cu $\sum$5(310) GBs [105]. For example, the B element can strengthen the connection of two grains while O-doped GBs show a weak feature. Although scientists have explored some alternative pathways for stabilizing GBs, a

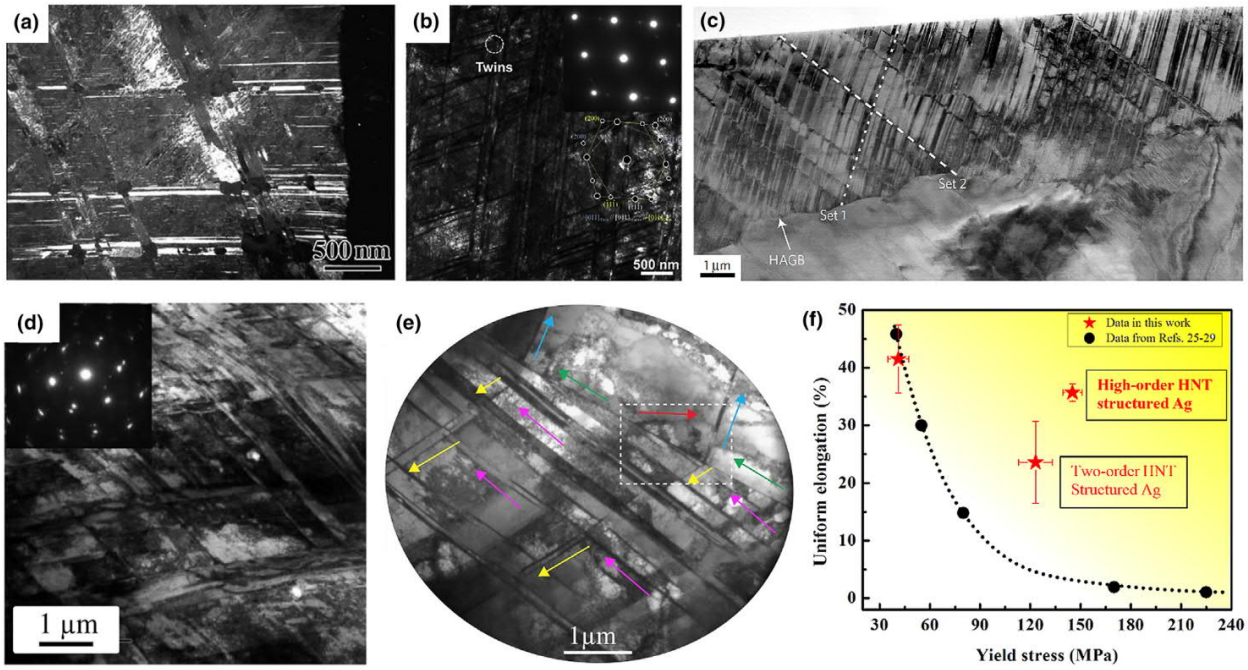

FIGURE 3

The examples of HNT structures in metals with good mechanical properties. (a) TRIP-gradient steels [22]. Copyright 2016, Elsevier. (b) TWIP steels [24]. Copyright 2018, Elsevier. (c) Additively manufactured austenitic 316L stainless steels [23]. Copyright 2017, Springer Nature. Sets 1 and 2 highlighted by white lines are two orientations of nanotwins. (d) Mo alloyed FeCoCrNi HEAs [28]. Copyright 2017, Elsevier. (e and f) High-order HNT Ag with superior strength and ductility [30]. Copyright 2018, Elsevier. Arrows in (e) highlight high-order nanotwins with different orientations.

comprehensive framework for these optimization strategies is far from achieved since the complexity of the interaction between different elements.

Strengthening by extreme grain refinement

Producing nano-laminated structure is an effective way for strengthening, where the lamellar thickness could be regarded as grain size [41]. As shown in Fig. 4b and c, the interface between two lamellae is a low-angle GB. The large fraction of low-angle GBs with good stability help Ni to achieve an ultrahigh hardness of ~6.4 GPa. The deformation is governed by dislocation and deformation twinning, which eventually leading to fragmentation of laminated structure into nano-sized grains [102]. Note that the finest laminated structures, with structural size of several nanometers, may also be stabilized by the low-energy boundaries and continue to strengthen nanocrystalline materials [43].

The grain size of Al can be tailored from ~130 to ~2 nm by controlling the addition of Fe solute [106]. The ultrastrong Al alloy (5.9 at.% Fe) is produced with 9R phase, nanotwins and extremely fine grain size of ~4 nm. The highest strength exceeds 1.5 GPa. On the other hand, the strengthening effect with extreme grain refinement can be maintained with the deformation under high pressure in nanocrystalline Ni [40]. Dislocation activity still can be induced with the grain size of ~3 nm and the strengthening effect is still dominated by the dislocation-GB interaction.

Recently, the simultaneous achievements of extremely fine grains and stabilization of GBs are realized in a Ni-Mo alloy [45]. The grain size is ~3.4 nm (Fig. 4d) and the hardness continuously rises when grain size below 10 nm (Fig. 4g). Instead of GB-mediated processes such as grain rotation and migration, the nucleation and propagation of extended partial dislocations dominate the deformation mechanism after Mo segregation and GB relaxation. Indeed, impurity segregation to the GBs can help with stabilizing nanograins, and thus reduce the critical grain size for inverse Hall–Petch effect. Another latest research progress is about pure nickel [107]. Instead of inverse Hall–Petch softening, the Hall–Petch strengthening effect extends down to a grain size of ~3 nm at high pressure (Fig. 4e). The YS for the nickel sample with a grain size of ~3 nm reaches ~4.2 GPa (Fig. 4h), which is ten times stronger than that of a commercial nickel material. The high-pressure condition changes the deformation mechanisms into both partial and full dislocation hardening instead of GB sliding induced softening due to excessive grain refinement. Note that such unusual compression strengthening behavior is also observed in gold and palladium, which indicates that it could be a novel approach to design high-performance nanostructural metallic materials. However, simultaneously manipulating the extreme grain refinement and GB stabilization is still challenging. For example, NT diamond with unprecedented hardness has been fabricated under high pressure and high temperature (Fig. 4f) [4]. However, the grain size is larger than 10 nm. Although the nanocrystalline diamond with grain size smaller than 10 nm can be synthesized, intergranular fracturing along poorly sintered GBs dominates the reduction of strength. Thus, the fabrication of extremely fine grains with well stabilized feature may lead to a significant increase of the hardness of diamond.

Previous theoretical models can describe grain refinement induced strengthening and softening (Hall–Petch relation and

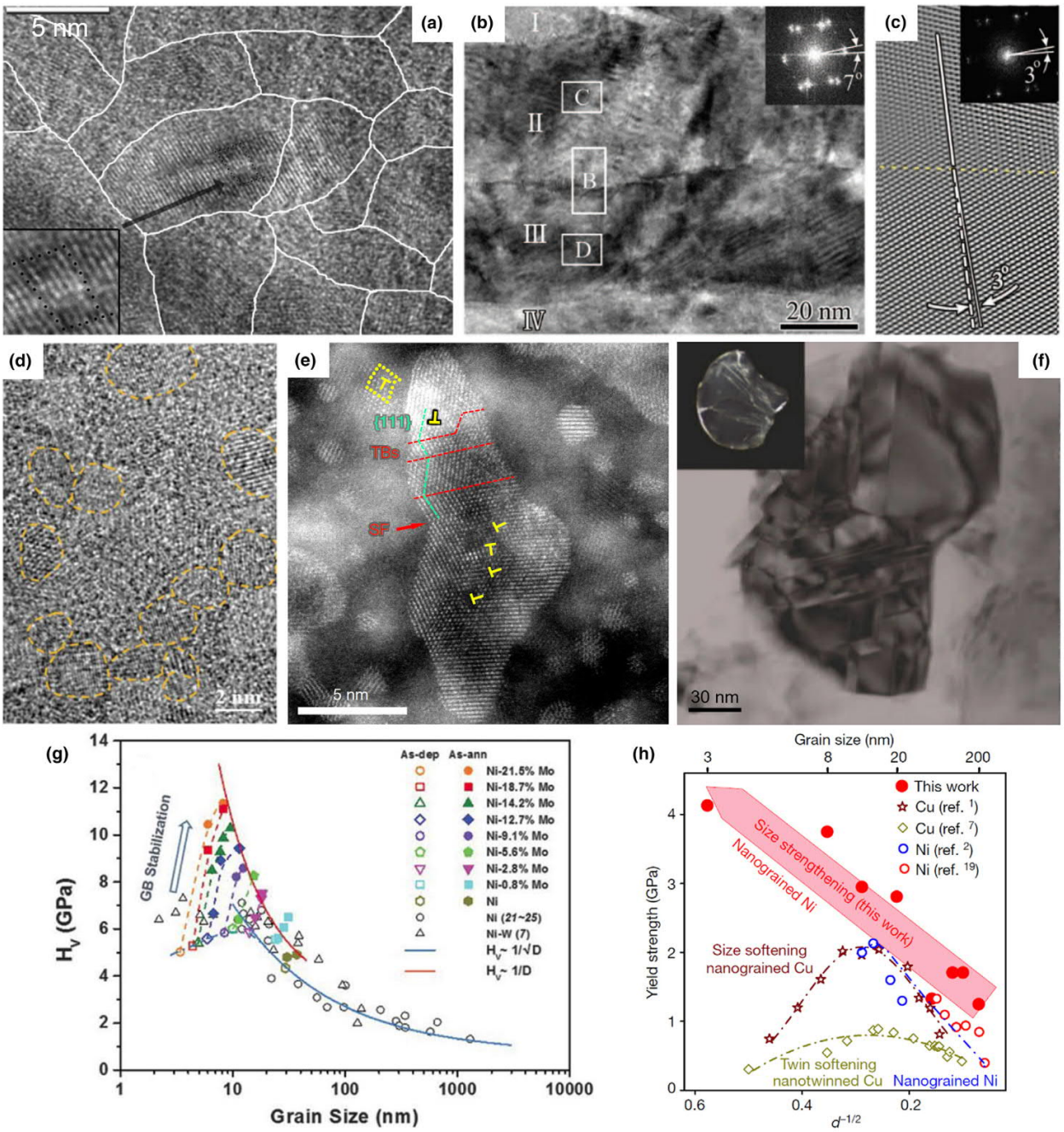

FIGURE 4

The examples of (extremely) fine grained nanostructures. (a) The dislocation based plasticity in nanostructured Cu with a grain size of ~5 nm [103]. Copyright 2014, American Physical Society. (b and c) The ultrastable nano-laminated structure with low-angle GBs in Ni [41]. Copyright 2013, AAAS. Labels I, II, III, and IV in (b) mark four lamellae. (c) is a Fourier-filtered image of the region 'B' in (b), showing a misorientation angle of 3° between lamella II and III. (d and g) The extremely fine grained Ni-Mo alloy (a grain size of ~3.4 nm) exhibiting an ultrahigh hardness by tailoring the stability of GBs [45]. Copyright 2017, AAAS. The dashed lines in (d) mark the extremely fine grains. (e and h) TEM observations of nickel samples quenched from 40 GPa with a grain size of ~3 nm and the extrapolated yield strength of nickel at ambient conditions without GB sliding versus grain size by elasto-viscoplastic self-consistent (EVPSC) simulations [107]. Copyright 2020, Springer Nature. Stacking faults (SFs), TBs and a few full dislocations can be observed in (e). *d* in (h) represents the grain size and twin thickness for nano-grained copper and nickel and NT copper respectively. (f) The NT diamond with the grain sizes technically limited over ~10 nm [4]. Copyright 2014, Springer Nature. The inset is a photograph of the transparent diamond (~1 mm in diameter).

inverse Hall–Petch effect) of nanocrystalline materials very well. However, the experimental studies reviewed in this section subvert the inverse Hall–Petch effect. Based on the newly discovered knowledge of the structural characteristics of nanostructures, it is essential to develop more reliable mechanism-based theoretical models, especially expected to be capable of predicting continuous strengthening or reverse softening for metallic materials with extreme grain refinement. We note that a mechanism-based plas-

ticity model is developed to describe GB sliding and diffusion behaviors of metals at high pressure [107]. It establishes a quantitative relationship between applied stress and the critical stress as well as grain size for the activation of GB induced plastic deformation. In addition, a modified Hall–Petch relationship is proposed, taking the effects of both full and partial dislocations into account. This new model reflects the effects of both full and partial dislocations, and can describe the size strengthening of metals over a wide size range.

Dislocation engineering

Dislocation, as a kind of defect, gives rise to a way for optimizing the properties of materials. The Taylor hardening law only specifies the strengthening effect by high dislocation density with the sacrifice of ductility. However, various dislocation morphologies have been observed with heterogeneous characteristics, which may improve the comprehensive mechanical properties. Hence, many researchers are motivated to engineer dislocation distribution and structures. They are mainly engaged in two aspects: (1) control dislocation morphologies and (2) unveil the relationship between dislocation patterns and mechanical performance.

Manipulation of dislocations

Solute segregation at dislocations is regarded as one of promising dislocation engineering method. Raabe et al. extended the planar complexion concept to linear complexion, emphasizing the importance of chemical and structural states at dislocations for nanostructural alloys [108]. For instance, the segregation of Nb atoms into dislocations are directly observed in ferritic stainless steels [53]. The segregation energy is almost the same as GB segregation energy, which implies that such segregation can be useful to retard the recovery of dislocations. The addition of Ca atoms promotes the accumulation of dislocations, which eventually transform into low-angle GBs and in turn Ca atoms and its precipitated substance segregate along low-angle GBs [55]. The segregation of carbon and Mn atoms to dislocations and GBs is clearly observed by atomic probe tomography (APT) (Fig. 5a), which is the prerequisite giving rise to the nucleation and growth of austenite [54]. On the other hand, the rate of austenite reversion can be accelerated by deformation because the deformation induced dislocations can accelerate the diffusion rate of solutes. Eventually, the transformation makes strained austenite into equiaxed grains [109]. In addition, hydrogen may not only reduce the nucleation and propagation force of dislocations but also activate additional slip planes [51]. Hydrogen can also accelerate Ni to form small dislocation cells and dense dislocation walls [52].

The dislocations with heterogeneous characteristics play an important role in the deformation behaviors of materials. The dislocation channels induce reverse ω-β transformation in TiNb-based alloys [58]. The dislocation cells and walls are observed in TWIP steels during tensile deformation (Fig. 5b) [60]. Fig. 5c shows the break of elongated dislocation cell boundaries during tensile deformation in martensite [66]. On the other hand, the heat treatment for medium-Mn TRIP maraging steel leads to the formation of austenite–martensite nanolaminate microstructure, with a high density of dislocations in α′ martensite matrix (Fig. 5d) [65]. Strain partitioning is governed by the interplay of dislocation slip, TRIP and TWIP effects during deformation. Moreover, carbon atoms and high dislocation density are employed to partition metastable austenite grains embedded in a highly dislocated martensite matrix (Fig. 5e) [66]. It is also reported that the addition of oxygen into certain HEAs can form ordered oxygen complexes [110]. They change the dislocation shear mode from planar slip to wavy slip, promoting double cross-slip and even dipolar dislocation walls are developed during deformation (Fig. 5f). Hence, the control of dislocations facilitates constructing inhomogeneous dislocation-based nanostructures. However, the nucleation dynamics of these nanostructures is complicated and require universal criteria.

Mechanical properties affected by dislocations

The as-extruded low-alloyed and rare-earth-free Mg alloys achieve ultra-high YS and UTS of ~443 MPa and ~460 MPa [55]. The strength and ductility can be balanced by adjusting the extrusion parameters, corresponding to the control of dislocation density and structures. In addition, a strong but ductile Mn-rich steel is produced with an increased warm ductility over 100% owing to a dislocation-accelerated austenite reversion during warm deformation [111]. Moreover, the nanoindentation hardness of austenitic stainless steel can be enhanced about 30% by the dissolved hydrogen [51]. Because the shear modulus is reduced with hydrogen charging, increasing the slip planarity for hardening by dislocations.

Ultralow-carbon martensitic steels show higher YS due to the tangled dislocations and dislocation cell structures by cold working [56]. Additionally, elongated α-Ti phase with high density of tangled dislocation cells is observed in Ti-6Al-4V alloy by asymmetric cryorolling, exhibiting a high UTS of ~1.1 GPa and an acceptable ductility of ~10.1% [111]. Dislocation walls strongly enhance the strain hardening behavior because its excellent capability of hindering dislocations [59]. Hence, the TWIP steels with dislocation substructures reach a high UTS of ~1.1 GPa and a large plasticity of ~50% [60]. Furthermore, a multistage hardening behavior is reported with the refinement of dislocation substructures, optimizing a steel with a superior UTS of ~1.6 GPa and a great ductility of ~55% [61].

On the other hand, the dislocation channels enable the strain localization at dislocation channels or the intersections with GBs [57]. Such localization triggers the phase transformation and forms partitioned structure [58]. The heat treatment leads to martensite-to-austenite reversion, which is the origin of strain partitioning during tensile deformation. It increases the uniform elongation from ~2.4% to ~17.1% while with little sacrifice of the YS and UTS from ~800 MPa to ~665 MPa and from ~925 MPa to ~900 MPa, respectively [65]. Moreover, by recovery annealing of austenitic stainless steel, the recovered mobile dislocations have a great contribution to the ductility of ~5.2% [49]. However, the YS of ~1055 MPa is not further improved although tangled dislocations and dislocation cells are observed, indicating such dislocation substructures formed during recovery annealing do not play a role in strengthening. It is also reported that an unprecedented combination of high YS and ductility of ~920 MPa and ~10% can be achieved for the ultrafine grained

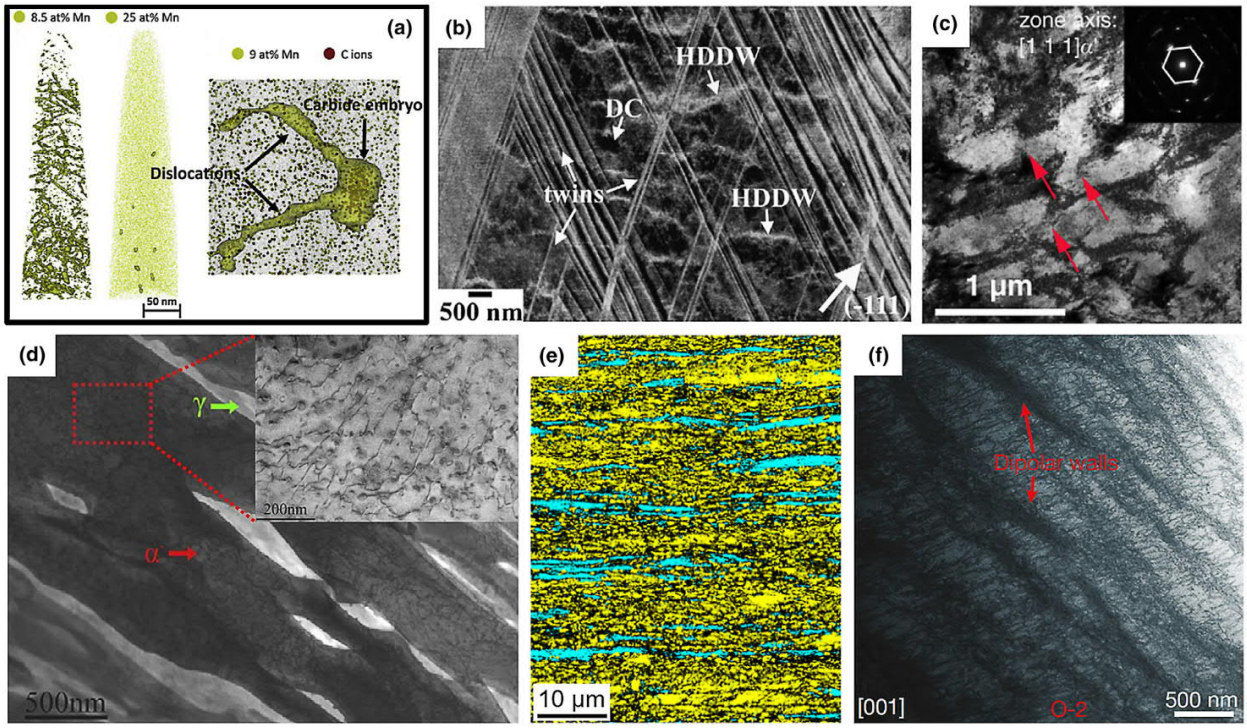

FIGURE 5

Dislocation distribution and structures. (a) Mn isosurfaces revealing the dislocations with Mn segregation, the small carbides nucleating in the dislocations and the carbide embryo being formed at the intersection of two dislocations in medium-Mn steel [54]. Copyright 2018, Elsevier. (b) Details of the dislocation substructure consisting of dislocation cells and high-density dislocation walls at a tensile strain of 30% in TWIP steel [60]. Copyright 2011, Elsevier. (c) The break of elongated dislocation cells after tensile straining in the tempered martensite matrix [66]. Copyright 2017, AAAS. (d) Duplex structure with nanoscale austenite (γ) finely distributed in the α' martensite matrix in medium-Mn TRIP maraging steel. The inset shows nanoprecipitates and high-density dislocations in α' martensite [65]. Copyright 2015, Elsevier. (e) The lamella austenite (light blue) embedded in tempered martensite matrix (yellow) [66]. Copyright 2017, AAAS. (f) STEM image of O-2 HEA at 8% tensile strain (the red arrows indicate the dipolar walls) [110]. Copyright 2018, Springer Nature.

316L steel [50]. It is pointed out that improved ductility is attainable by reducing the dynamic dislocation recovery rate.

Recently, a new kind of deformed and partitioned steel is developed with high dislocation density, exhibiting a high YS of ~2.21 GPa and a uniform elongation over ~15% [66]. Besides the contribution of high dislocation density, dislocation cell and wall structures, high YS is also assisted by solid solution, precipitation, twinning, grain refinement and strain partitioning. Intriguingly, the ductility also comes from the high dislocation density. The good ductility is ascribed to the glide of intensive mobile dislocations and the TRIP effect. A breakthrough outcome for HEAs is reported with both great YS of ~1.11 GPa and elongation of ~27.66% [110]. The ordered oxygen complex, which induces a large density of dipolar dislocation walls assists the excellent mechanical properties. Hence, comprehensive exploration of dislocation-based strengthening and ductilizing mechanisms provides the opportunity to breakdown the strength-ductility trade-off of materials. In terms of theoretical modeling of dislocation structures such as dislocation channels, cells and walls, traditional dislocation theory cannot describe the additional enhancement of materials by the complicated dislocation structures. Not only dislocation density but also dislocation structures should be taken into consideration for the development of dislocation-based theoretical models.

Gradient grain refinement

Gradient grained structure is generally produced by several gradient deformation pathways such as surface mechanical grinding treatment (SMGT), surface mechanical attrition treatment (SMAT) and surface rolling. It may also induce the gradient of dislocations, twins and stacking faults (SFs) etc. The microscopic structural divergence of materials alters the macroscopic mechanical performance due to the non-uniform deformation behavior. The synergy of great strength of nano-grained region and the good ductility of coarse-grained region promotes high strength and high ductility of metallic materials.

Mechanical performance

The gradient structure is first successfully fabricated in copper [35]. The gradient nano-grained film exhibits a YS of ~660 MPa, 10 times higher than that of coarse-grained counterpart but with a small uniform elongation of <2%. However, the combination of gradient nano-grained surface layer and coarse-grained substrate in copper samples can obtain a YS of ~129 MPa, twice higher than coarse-grained copper, and a large uniform elongation of ~31%. The design of gradient nano-grained layers is also effective in steels [36]. Gradient nanostructure provides an effective approach to leap out of the traditional

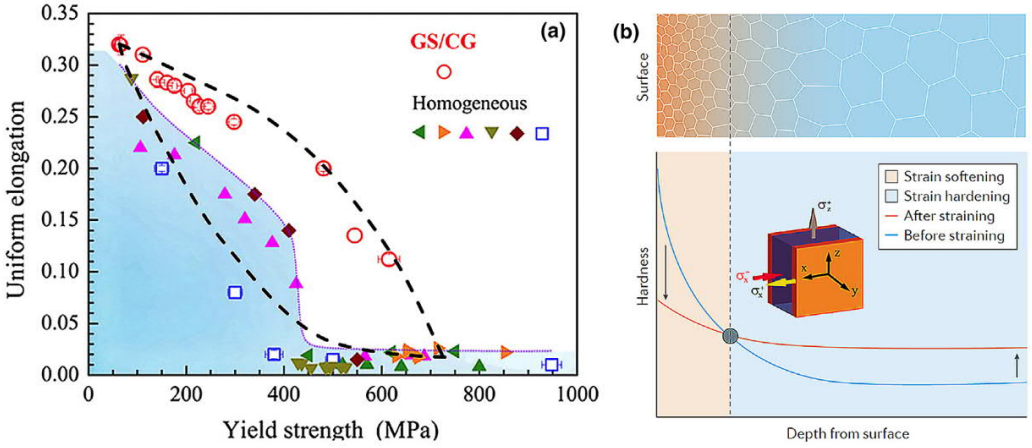

FIGURE 6

(a) The strength and ductility of gradient grained steel compared with their homogeneous counterparts [36]. Copyright 2014, National Academy of Science. (b) Schematic representation of a sample with a gradient grained structure and variation of the hardness as a function of the depth from the surface before and after straining [43]. Copyright 2016, Springer Nature. The inset of (b) shows the schematic stress state change during uniaxial tension in a gradient grained structure [36]. Copyright 2014, National Academy of Science.

"banana curve" for the trade-off between strength and ductility (Fig. 6a). The gradient architecture exhibits a large uniform elongation while the YS is of ~2.6 times higher. Gradient grained structure is also synthesized in nickel by direct-current electrodeposition [112]. The YS, UTS and uniform elongation for such gradient grained nickel are ~687 MPa, ~1094 MPa and ~4.5% respectively. The total elongation reaches ~ 11% and an exceptional crack-growth toughness of 200 MPa.m½ is achieved. The gradient-grained nickel displays a much-improved combination of high strength and toughness compared to uniform grain-sized nano-grained or coarse-grained counterparts.

Furthermore, gradient architecture can be combined with other advanced strategies. For instance, the mutual effect between TRIP and gradient grain distribution in austenite stainless steels can further increase the plasticity and simultaneously maintain high strength [22]. The YS of ~1.5 GPa and the flow stress of 2 GPa are achieved during tensile deformation and the uniform elongation is over 20%. On the other hand, the gradient structure with TWIP effect can further improve the strength and ductility [19,20]. The SMATed steel maintains an ultrahigh YS of ~2 GPa and a uniform elongation of ~15%. The YS of pre-torsioned steel is doubled without the sacrifice of ductility, which is attributed to the gradient HNT structure. Moreover, an extra strengthening and work hardening effect is realized in gradient NT copper, with an ultrahigh YS of ~485 MPa and a uniform elongation of ~7% [113]. The successful combination of advanced gradient and NT structures boosts this impressive achievement. Hence, efficiently adopting various strategies may further subvert the traditional strength-ductility dilemma.

Strain delocalization and hardening

The poor ductility of nano-grained metals is mainly attributed to the lack of work-hardening behavior and hence results in the early strain localization and failure. Accordingly, gradient structure can suppress the early occurrence of strain localization. Because the gradient structure alters the deformation mechanism to mechanically driven growth of nano-sized grains [35]. Besides, the gradient structure exhibits elastically homogeneous but plastically heterogeneous characteristics, which leads to a macroscopic strain gradient. The strain gradient converts the uniaxial stress to multi-axial stresses owing to the incompatible deformation (the inset of Fig. 6b), which enables strain delocalization and work hardening from coarse-grained region. Therefore, the special stress distribution may enhance the nucleation and propagation of dislocations and induce an extra strain hardening [36]. Specifically, three deformation stages during uniaxial tensile deformation of gradient grained metals have been revealed [114]. In Stage I, the gradient grained materials deform elastically. In Stage II, the coarse-grained central layer begins to deform plastically while the nano-grained surface layers still deform elastically. Such incompatibility converts the uniaxial stress into bi-axial stresses. Furthermore, two elastic/plastic interfaces exist and move toward surface with the increase of applied strain. And stress and strain gradient appear, contributing to a synergetic strengthening and back stress to raise the yield strength. In Stage III, both coarse- and nano-grained layers deform plastically. Unstable necking first occurs in the nano-grained layers. However, necking is constrained by the stable coarse-grained layer. A steep strain gradient occurs near the interfaces of the necking layers and the central stable layer, promoting strain hardening capability via the accumulation of geometrically necessary dislocations and back stress. In addition, the necking/stable interfaces migrate from surfaces toward the central layer, accompanied by the accumulation of high density of dislocations, enhancing strain hardening rate and thus, improving the ductility of gradient grained materials.

The inconsistent deformation behaviors lead to the mechanical incompatibility. The hardness can be redistributed after straining (Fig. 6b) [43]. The dislocation induced hardening in coarse-grained layer and GB migration induced softening in nano-grained layer are activated concurrently in gradient structure. Moreover, the great strain hardening capability also comes from the generation of abundant geometrically necessary dislocations in gradient grained layers due to the non-uniform defor-

mation [37]. The strain hardening rate of gradient structure could be as high as coarse-grained counterpart. By virtue of the superior strength of nanograins, good ductility of coarse grains and gradient distribution, strain delocalization and extra strain hardening are achieved to develop strong and ductile materials. Moreover, with the combination of gradient and NT structures, a large structural gradient allows for superior work hardening and strength because the dislocation density can be tuned toward an ultrahigh level [113]. Thus, the synergy of various gradient types such as grain size gradient, twin density gradient and dislocation gradient provides a pathway for excellent strength-ductility design.

To quantitatively describe the structure–property relation of gradient metallic materials, a series of theoretical models have been developed. A dislocation density-based theoretical model is developed to quantitatively investigate the mechanical behaviors and properties such as the yield strength, ductility as well as the strain hardening of gradient grained metals [37,115,116]. A dislocation mechanism-based crystal plasticity model is developed to describe the size-dependent mechanical behavior of gradient grained materials [117]. Besides, Zhao et al. develop a multiple mechanism-based constitutive modeling of gradient grained material to evaluate the contribution of various strengthening mechanisms to gradient grained materials [118]. Furthermore, Zhu et al. develop theoretical models to describe the effect of gradient grain size, bimodal grain distribution and gradient nanotwinning simultaneously on mechanical behaviors of gradient-nanostructured materials [119–122]. Based on the understanding of the underlying mechanisms contributing to the improved strength-ductility synergy, quantitative optimization strategies for the mechanical properties of gradient grained materials could be achievable.

Nanostructured metallic glasses

Metallic glasses (MGs) are a class of metallic materials with disordered arrangement of atoms, which is totally different from crystalline materials that showing periodic lattice structure. The excellent strength of MGs has long been reported. However, the poor ductility of MGs limits their application. Many researchers are engaged in improving the ductility of MGs, in which tuning the nanostructures of MGs has been identified to be an effective pathway.

Microstructure of nanostructured MGs

Through physical vapor deposition via magnetron sputtering, nanostructured MGs have been synthesized as thin film materials in a variety of binary or multi-component alloy systems such as Au-La, Fe-Si, La-Si, Pd-Si, Ni-Ti, Ni-Zr, Sc-Fe, Ti-P Fe-Sc, Pd-Si, Zr-Pd, Ti-Zr-Cu-Pd, Cu-Zr-Al, Co-Al-Y-Ti and Au-Ag-Pd-Cu-Si-Al [74]. As demonstrated in Fig. 7a [74], a typical nanogranular structure is clearly characterized by scanning electron microscope (SEM) for an Au-based nanoglass MG (NGMG). Moreover, the transmission electron microscopy (TEM) micrograph (Fig. 7b) confirms the formation of nanostructure with an average nanogranule size of about 30 nm, of which the amorphous nature is further verified by selected area electron diffraction (SAED) (the inset of Fig. 7b).

To further examine the structural characteristic of the Au-based NGMGs in more detail, Chen et al. [123] have carried out high resolution TEM (HRTEM) experiments as well. Studies on HRTEM images observed maze-like patterns, that is typical for an amorphous structure and thus both the nanograins and the grain interfaces are confirmed to be glassy (Fig. 7c). In addition, the nano-beam electron diffraction (NBED) patterns (Fig. 7d and e) from the nanograins and interface structure illustrate only a diffuse halo, also evidencing the amorphous nature. However, it is interesting that the diffuse halo from the interfacial region is remarkably broadened compared with nanograins, implying the relatively less atomic-scale short range orders or less dense atomic packing in the interface structure (Fig. 7d and e). In the previous investigations, more compelling evidence for the local variation of atomic-scale structure in nanostructured MGs has also been found by means of the wide angle X-ray diffraction [124]. The nanoglass and melt-spun glass are with the same chemical compositions. The coordination number in the glass-glass interfaces (GGIs) is reduced by about 20% compared to those of melt-spun glass and the glassy grains of the nanoglass (Fig. 7f). As indicated by Moessbauer spectroscopy, a volume fraction of 35% of GGIs exists in the granular structure of $Sc_{75}Fe_{25}$ nanoglass produced by consolidating $Sc_{75}Fe_{25}$ glassy clusters at a pressure of about 4.5 GPa [81].

Mechanical properties of NGMGs

Based on the previous experimental and computer simulation studies, it has been shown that NGMGs, a new type of amorphous materials with inhomogeneous microstructure, consist of nanometer-sized glassy regions interconnected by GGIs [73,74]. In particular, the atomic structure in these interfacial regions with a reduced packing density differs from the ones in the glassy regions, which usually results in a large structural heterogeneity (or free volume) which is uncommon in conventional MGs obtained by rapidly cooling of supercooled metallic liquids. By comparison, the trigger of shear band associated with rearrangements of group of atoms, i.e. shear transformation zone (STZ) upon loading is easier in NGMGs because of the existence of GGIs. On the other hand, the propagation of shear bands can however be pinned or bifurcated by the surrounding harder glassy granules, preventing the material from catastrophic failure even in tension testing. As a result, multiple shear bands form in the nanostructured MGs, leading to remarkable plastic strain even under tensile condition. For example, by performing in-situ TEM compressive and tensile tests on NGMGs and melt-spun $Sc_{75}Fe_{25}$ MGs, Wang et al. [79] found that the nanostructured samples exhibit large plasticity, whereas the melt-spun MGs with monolithic microstructure usually fail without a significant plastic strain. As illustrated in Fig. 8a, a distinct plastic yield can be observed following the initial linear elastic deformation for a 300 nm nanoglass. When the test stopped at a preselected strain of 50%, the sample had undergone a strain of ~43% in the axial direction and ~35% in the transverse direction (Fig. 8b). By comparison, the monolithic MG pillar exhibited purely elastic behavior and a dramatic stress drop, followed by another catastrophic stress drop (Fig. 8a and c).

Furthermore, the tensile plastic strain of the NGMG is remarkably enhanced to as high as 15% in contrast to the conventional

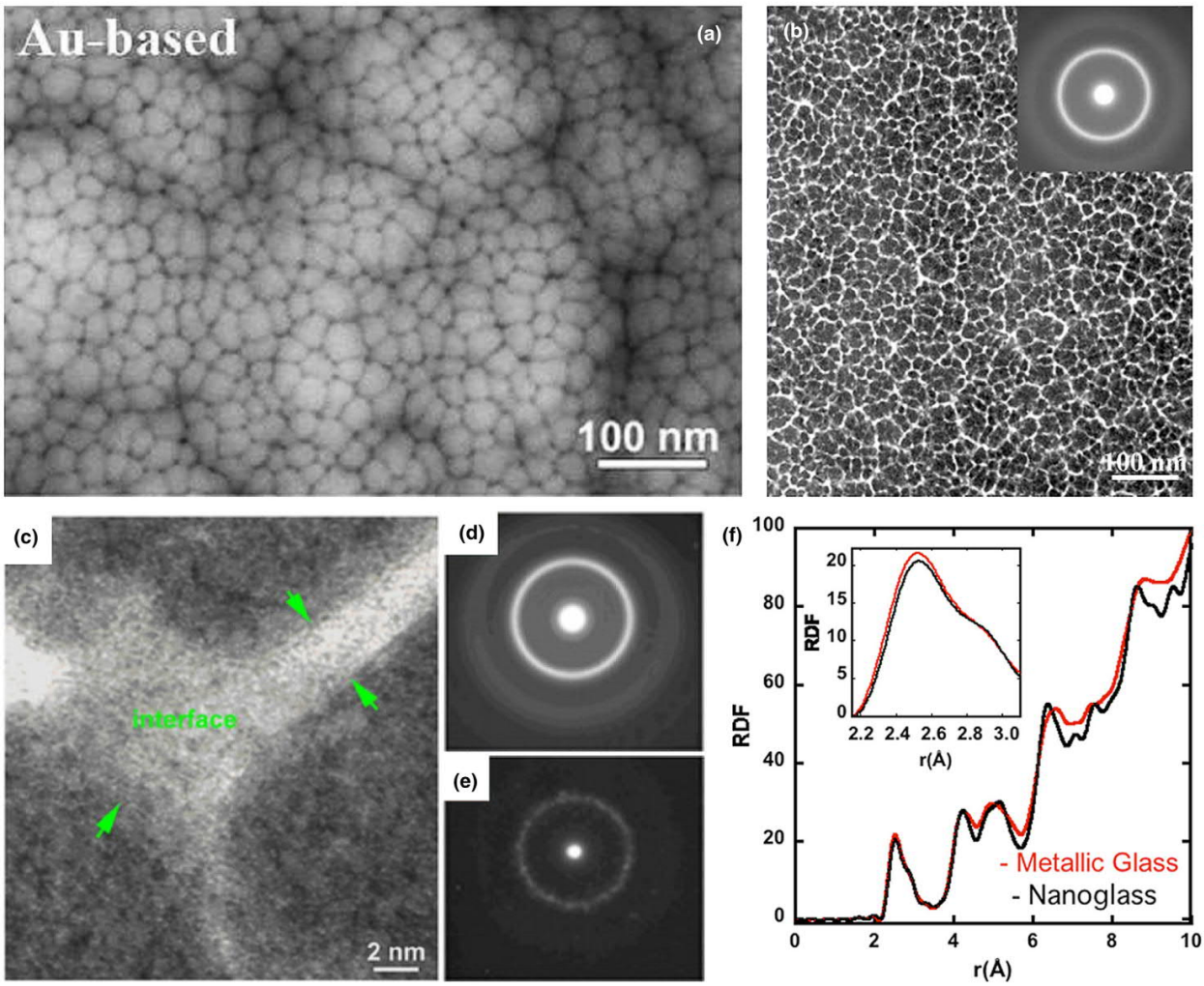

FIGURE 7

(a and b) The SEM and bright-field TEM images showing the surface morphology of an Au-based NGMG synthesized by inert gas condensation. The inset in (b) is the corresponding SAED pattern [74]. Copyright 2017, Elsevier. (c) HRTEM image illustrating the interfaces between glassy particles [123]. Copyright 2013, IOP Publishing. (d and e) The typical nanobeam diffraction (NBD) patterns of the GGI and glassy nanograins, respectively [123]. Copyright 2013, IOP Publishing. (f) Comparison of the radial distribution function (RDF) of the melt-spun MGs and NGMGs of $Fe_{90}Sc_{10}$ [124]. Copyright 2012, AIP Publishing.

glassy alloys with same chemical composition, while the significant necking phenomenon can be observed (Fig. 8d and 8e). Additionally, the rotation and/or stretching of glassy grains during deformation might also contribute to the tensile ductility for this new amorphous metallic materials [74].

Size effects on mechanical properties of NGMGs

For polycrystalline alloys, granular size has been known to be one of the essential factors controlling their mechanical behaviors. Typically, the strength of polycrystalline materials increases with the decrease of grain size. In view of this, it is very interesting to examine the interior length scale effects on the mechanical properties of NGMGs since it possesses a unique nanogranular structure. According to MD simulations [78], the granular size does play an important role on strength of NGMGs. The smaller the nanogranules, NGMGs become softer and then ductile. That is, an inverse Hall–Petch effect emerges as the granular size falls into the range of a few to several tens of nanometers. Moreover, below a critical grain size, NGMGs are found to gradually undergo homogeneous deformation instead of inhomogeneous one.

Experimentally, by performing in-situ micropillar compression tests on a NGMG, it is reported by Wang et al. [125] that the sample size can significantly affect their YS and deformation mode (Fig. 9a and b). Owing to the intrinsic length scale related to the plasticity initiation, one can observe the increase of YS with the decrease of sample size from ~300 nm to ~100 nm (Fig. 9a). When the sample size further reduces to 100 nm or below, it becomes very difficult for shear band nuclei to grow into shear bands on account of the limited free space in the nanometer-scale samples. Consequently, the nanoglass exhibits a uniform deformation associated with multiple shear bands during the compression tests (Fig. 9a and b). The interfacial region with reduced density (or excess free volume) serves as a preferential site for the initiation of embryonic shear band, which can develop into mature shear band when a critical incubation size

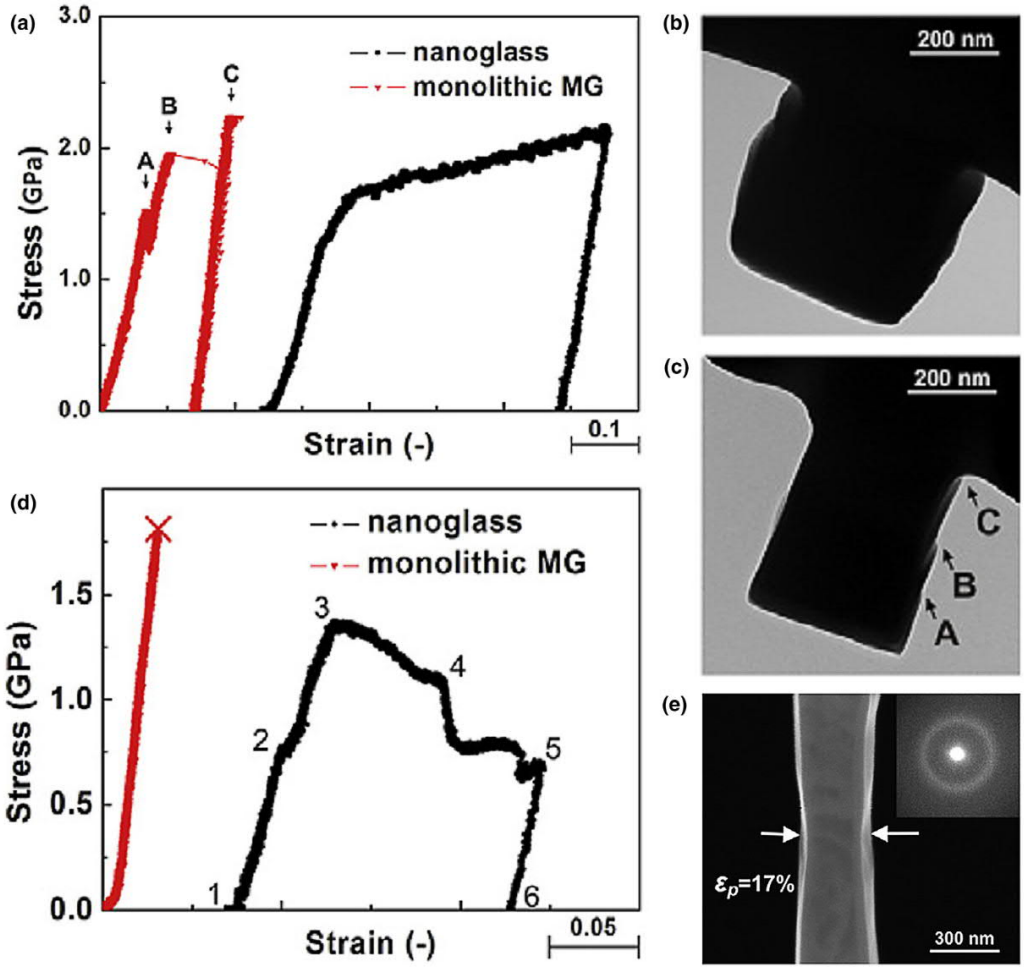

FIGURE 8

Mechanical tests of Fe-Sc nanoglass and the monolithic MG [79]. Copyright 2015, Elsevier. (a) The compressive stress–strain curves obtained from micro-compression tests. The post-morten TEM images of (b) NGMG pillar and (c) monolithic MG pillar. The stress drops marked by A, B, C in (a) correspond to the shear offset appearing on the free surface of pillar in (c). (d) The tensile stress–strain curves of the nanoglass and monolithic MGs. (e) The frames extracted from the recoded movie for the Fe-Sc NGMG, showing the occurrence of plastic deformation during the in-situ tensile in TEM (the inset of (e) is the corresponding SAED pattern).

scale l_{inc} is reached (Fig. 9c and 9d). Hence, exploiting the nanostructures of MGs shed a light on the improvement of comprehensive mechanical properties.

Nevertheless, it is worth noting here that the Fe-Sc nanoglass samples studied respectively by Gleiter et al. [72] and by Wang et al. [79] show a similar ductility but are seen to vary dramatically in the shape and GGI thickness in the nanoglassy structure. Therefore, it indicates that there should be another key factor, e.g. nanoglassy grain size, controlling the plastic deformation of Fe-Sc nanoglass. The size effect of crystalline metal is ascribed to the interplay between the intrinsic size such as the grain size or twin spacing and the extrinsic size such as the sample size or deformation field [126]. Despite the lack of crystalline defects, MGs also exhibit similar strength size effect, which has been rationalized as size-dependent shear band nucleation that involves a critical length scale triggering the autocatalytic growth of nanosized shear band embryo [127,128].

In theory, one can envision that if the ductility of a MG is associated with the shear banding-induced plastic deformation, a larger critical length scale is anticipated for the initiation and/or propagation of embryonic shear band, leading to a distributed shear banding rather than shear instability that causes catastrophic failure [126,129]. The nano-scale glassy grain is beneficial for the nucleation of homogeneous-like shear band when its size is smaller than the critical length scale. Based on this model, the size reduction induced ductility observed by Greer et al. [130] can also be reasonably interpreted. For example, when the sample size is small enough, a sample surface effect would come about once the local plastic zone, e.g. STZ or shear band nuclei grows to a sample surface before reaching the critical length scale for macroscopic shear instability.

Since shear banding behavior is one of the most important deformation characteristics for MGs, many efforts about theoretical modeling have been made to quantitatively describe shear banding and thus, figure out the structure–property relation of MGs. For example, a coupled thermo-mechanical model is proposed with the consideration of the momentum balance, the energy balance and the dynamics of free volume [131]. In addi-

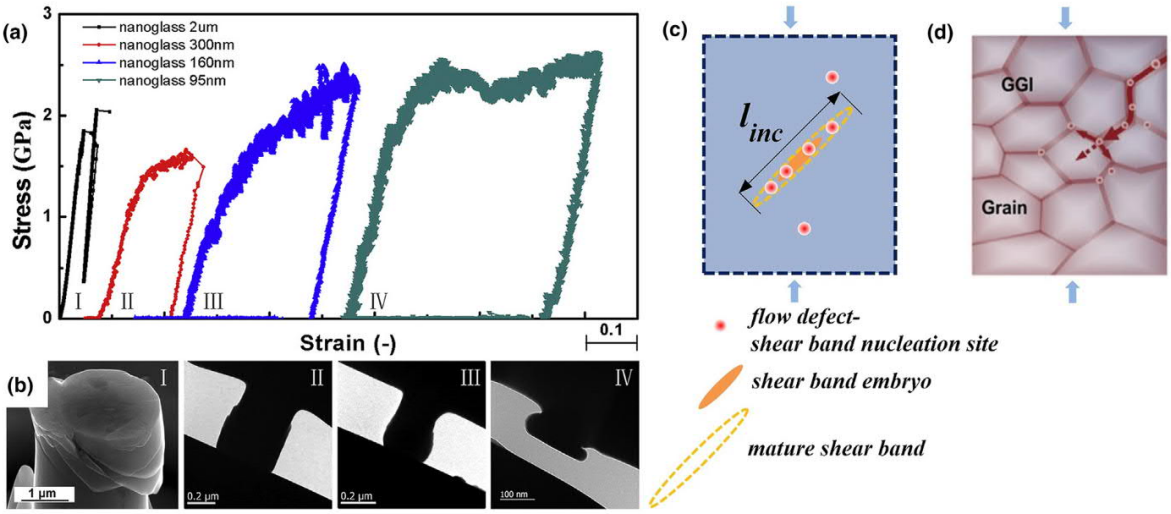

FIGURE 9

Mechanical tests and Schematic representation of shear band nucleation for NGMG [125]. Copyright 2016, Elsevier. (a) The compressive stress–strain curves for $Sc_{75}Fe_{25}$ NGMG pillar. (b) The frames are extracted from recorded movies for (I) 2 μm; (II) 300 nm; (III) 160 nm; (IV) 95 nm NGMG pillars, respectively. (c) Schematic illustration of shear band nucleation and formation in NGMG: as the requirements for quantity and orientations have been reached, a series of flow defects will develop into a mature shear band in NGMG sample. l_{inc} represents a critical incubation size scale for mature shear band. (d) The existence of a large number of GGIs benefits for shear band nucleation and the subsequent multiple shear banding in the NGMG.

tion, a non-local and finite-deformation-based constitutive model is developed to study the size effect of shear localization process observed in experiments [132]. In recent years, the non-local constitutive model is further developed to analyze the ductility enhancement mechanism of NGMGs [78] and the tensile deformation of NGMG-MG laminate composites [133]. The progress for theoretical modeling of NGMGs is still very limited, which may be attributed to the complexity of amorphous structure. Using experimental characterization and MD simulation approaches to deepen the understanding of key microstructure information may promote the development of constitutive models for NGMGs in future.

Supra-nano-dual-phase nanostructuring

The material strengthening methods are usually known as 'grain/interphase boundary strengthening', 'twin boundary strengthening', 'solid solution strengthening' and 'precipitate or dispersed reinforcement particle strengthening', of which the 'grain/interphase boundary strengthening' is most widely used. In this section, a series of special dual-phase nanostructured materials with the structural unit sizes below sub-10 nm are introduced. The intrinsic size effect greatly changes the mechanical behaviors of materials.

Supra-nano-dual-phase glass-crystal (SNDP-GC) metallic materials are composed of nanocrystalline and glassy phases. The length scale effects of crystals and MGs influence the mechanical behaviors and properties of SNDP-GC materials. The in-depth studies unveil that compared to the nano-sized structural units (<100 nm), the mechanical behaviors and properties of materials with the structural units between 1 nm and 10 nm are totally different. Superior mechanical properties of many new nanostructural metallic materials benefit from the structural units within the size range of 1∼10 nm. Thus, we propose a new term of 'supra-nano' to describe this family of new nanostructural metallic materials, referring to the materials having structural units within 1∼10 nm.

Supra-nano classifies a generic size zone of microstructures to achieve excellent mechanical property. Multiple phases of supra-nano sized MGs and crystals could be tuned to design high-performance materials. To date, five representative types of SNDP nanostructures have been observed. As summarized by a series of brief schematic diagrams shown in Fig. 10, *Type 1* is composed of supra-nanocrystal **&** supra-nano glass; *Type 2* is composed of supra-nano glass **&** glass-glass interface, with different atomic packing structure and/or composition; *Type 3* is composed of supra-nano glass **&** supra-nano glass, with different atomic packing structure and/or composition; *Type 4* is composed of supra-nanocrystal **&** secondary element/structure enriched GB; *Type 5* is composed of supra-nanocrystal **&** supra-nanocrystal, with different crystalline structure and/or composition. Note that the attainable SNDP nanostructures may not just be limited to these types. Hereafter, five representative examples are briefly introduced corresponding to five types of SNDP nanostructures.

A Mg-based SNDP-GC [71] reported in the year 2017 is *type 1*. This magnesium-based alloy exhibits an ultrahigh strength of 3.3 GPa, reaching the near-ideal strength of $E/20$, where E is the Young's Modulus of the material. As shown in Fig. 11a, researchers used a secondary supra-nano amorphous phase to replace the ordinary GB structure, which shows 6-nm $MgCu_2$ nanograins dispersed uniformly in the $Mg_{69}Cu_{11}Y_{20}$ amorphous matrix, with a nanocrystal volume fraction of ∼56%, revealing the MG/nanocrystalline dual-phase structure. In this way, the GB sliding/rotation mechanism of the supra-nanocrystals is impeded. Instead, the deformation mechanism of this Mg-based SNDP-GC is the multiple embryonic shear banding associ-

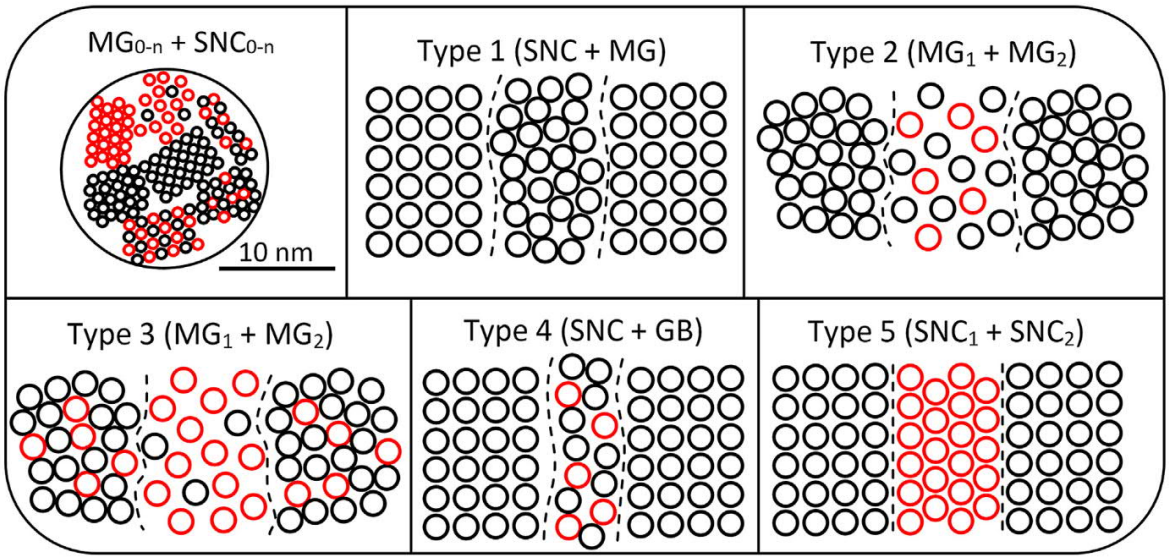

FIGURE 10

The schematic diagrams of supra-nano (all phases with the intrinsic length scale smaller than 10 nm), and five representative types of SNDP nanostructures synthesized in experiments. "SNC" is the abbreviation of "supra-nanocrystal". Black and red circles represent different elements.

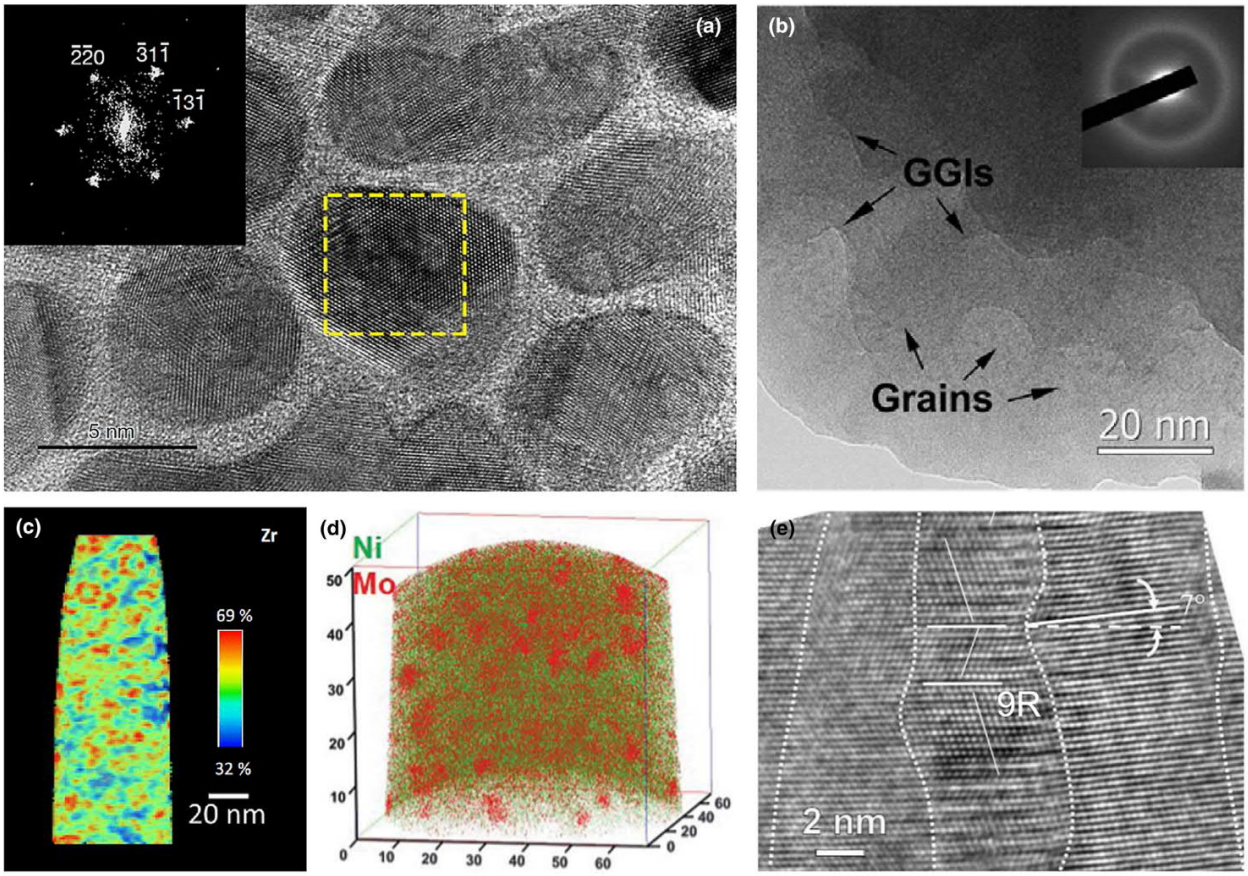

FIGURE 11

(a) HRTEM image of the Mg-Cu-Y SNDP-GC [71]. Copyright 2017, Springer Nature. The inset is an FFT image of the $MgCu_2$ nanocrystal marked by the dashed line, oriented to the [114] zone axis. (b) HRTEM image of the Sc-Fe nanoglass [79]. Copyright 2015, Elsevier. The inset is the SAED pattern recorded from the region shown in (b). (c) APT image of the Cu-Zr nanoglass showing segregation of Zr in the range of 5–6 nm [135]. Copyright 2017, Elsevier. (d) APT image of the Ni-14.2 at.% Mo alloy showing distributions of Ni and Mo in the sample annealed at 500 °C [45]. Copyright 2017, AAAS. (e) Microstructure of the Al-5.9 at.% Fe alloy showing high-density 9R, coherent twin boundaries (CTBs) and SFs [106]. Copyright 2018, John Wiley and Sons.

ated with division and rotation of the nanocrystals. Note that some of the crystal-crystal interfaces of SNDP-GC alloy seem not to be amorphous (Fig. 11a). This is mainly caused by TEM sample thickness effect that some of the crystal-crystal interfaces are not in edge-on condition. Therefore, a large volume fraction of crystals induces crystal overlap. In fact, the amorphous phase keeps a maze-like pattern.

In the year 2015, from a view of length scale, a Sc-Fe NGMG reviewed above is composed of ~10 nm sized glassy grains and ~1 nm thick GGI (Fig. 11b) [79], which can be seen as SNDP *type 2*. The 400 nm Sc-Fe nanoglass exhibits a plastic strain of ~15% under uniaxial tension, which is unprecedented among MGs of similar sample size. The outstanding plasticity of the nanoglass is originated from sub-embryonic shear bands generated from the GGIs. The detailed deformation mechanisms have been introduced in the previous content. The homogeneous flow of MG usually appears only below the size of 100 nm [134]. By supra-nanostructure design, the critical size for homogeneous plastic deformation surprisingly increased to 400 nm.

In the year 2017, a Cu-Zr nanoglass composed of Zr-enriched and Cu-enriched regions with the size of ~6 nm was fabricated by magnetron sputtering assisted inert gas condensation method (Fig. 11c) [135], which can be regarded as SNDP *type 3*. Homogeneous deformation was observed in nanoglasses during indentation whereas the melt-spun ribbons deformed by shear bands. The homogeneous deformation is attributed to high free volume in supra-nano GGIs. It has been reported that under indentation, mature shear banding behavior prevails plastic deformation for MG, which results in either localized 10~20 nm-thick shear bands or crystallized nanocrystals near the shear bands. GGIs turn mature shear banding behavior into homogeneous plastic deformation for MG. The homogeneous deformation of Cu-Zr nanoglass will provide profound implications in high impact and wear circumstances.

In the same year, the aforementioned extremely fine grained Ni-Mo alloy which is composed of supra-nanocrystals and Mo segregated GBs was fabricated by direct current electrodeposition and heat treatment (Fig. 11d) [45], which can be regarded as SNDP *type 4*. The stabilized GBs prevent the softening effect of supra-nanocrystals and promote the alloy to achieve an ultrahigh hardness of 11.35 GPa. Such SNDP nanostructure subverts the reverse Hall–Petch effect. The GB softening effect is eliminated successfully. In Ni-Mo alloy, Mo segregated in the GBs after annealing, which changes the lattice parameters and thus, overcomes the GB sliding/grain rotation related softening owing to GB stabilization. Therefore, by tailoring GBs at supra-nano scale, the Hall–Petch relation is also effective even below the grain size of 10 nm.

In the year 2018, a NT Al-Fe alloy with 9R phase composed of ~4 nm sized columns was fabricated by magnetron sputtering (Fig. 11e) [106], which can be regarded as SNDP *type 5*. The distorted 9R phase facilitates strain hardening and compensates the grain coarsening induced softening upon loading, which results in a plateau ultrahigh true stress of more than 1.5 GPa during compression.

Fig. 12 shows the development milestones of the structural alloys in the 21st century. It shows that researchers have paid efforts to increase the strength of alloys. The advanced strategies include nano-gradient structure design [136], nanotwinning [2,106] or hierarchically nanotwinning [19], nanoparticle [137,138] or nanoprecipitation reinforcement [90], dislocation engineering [66], GB engineering [45] and SNDP nanostructuring [71]. Some strategies are employed to fabricate materials with high strength as well as good ductility, and others effectively improve the strength to an ultrahigh value. The development of new materials become very fast (especially from 2014 as shown in Fig. 12). We do believe that more supra-nano materials will be developed in the near future via the smart combination of supra-nano crystalline and/or glassy phases.

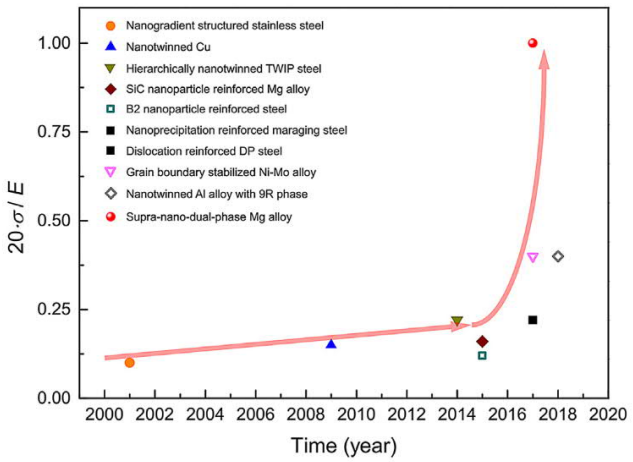

FIGURE 12

Development of high strength structural alloys in the 21st century. The strengths (σ) of the materials are compared with their near-ideal value $E/20$ (E is the Young's modulus of a material).

SNDP nanostructures could be regarded as a series of composite structures. In fact, many theoretical models have been developed to describe the mechanical behaviors and properties of composite metallic materials, in which MG matrix composites are paid much attention because the inclusion of toughening crystalline phases into MG matrix can improve the plasticity of MGs (crystalline/amorphous dual-phase). For example, based on the extended free volume model and unified visco-plastic model for MGs and crystals respectively, a meso-mechanical constitutive model is proposed to predict the tensile and compressive deformation behaviors of MG matrix composites with toughening phases [139]. A modified thermo-mechanical coupled constitutive model is developed to predict the effects such as the volume fraction and mechanical properties of particles and strain rate on the mechanical behaviors and properties of MG matrix composites [140]. Utilizing free volume model and Ludwik flow equation for MGs and crystals respectively, a micromechanical multi-phase model is developed to address the mechanical behaviors of MG matrix composites, with the consideration of TRIP effect [141]. On the other hand, based on strain gradient theory, a micromechanical model is proposed to simulate the stress–strain relationship, strain hardening rate and creep strain rate of dual-phase equiaxial nanocrystalline Ag-Cu alloy (crystalline/crystalline dual-phase) [142]. Although the theoretical models have been verified to be effective for the description of the composite structures that similar to SNDP

nanostructures, the special supra-nano length scale significantly changes the mechanical behaviors of SNDP materials compared with the conventional composite ones. Thus, these theoretical models may need further development to accurately describe the mechanical behaviors for each phase alone as well as the interaction between phases at supra-nano scale.

Other strategies for high-performance structural materials development

Nanoprecipitation

The formation of nanosized precipitates is one of the favorable approaches to improve the mechanical performance of materials. Because the nanoparticles can impede and accumulate dislocations or other defects, enabling work hardening. Such strategy has been employed to produce high-performance steels. For example, the nanoprecipitate-hardened high-strength steels achieve a UTS of 1.3∼1.5 GPa and an unexpected good total elongation of 10∼21% [143]. In particular, the increased elongation is attributed to the nanoprecipitates which trigger the Orowan hardening mechanism. Recently, a kind of steel with high-density nanoprecipitates exhibits an ultrahigh strength of ∼2.2 GPa and good ductility of ∼8.2% [90]. The lattice misfit between the nanoprecipitates and the surrounding matrix is minimized, decreasing the nucleation barrier for nanoprecipitation. Besides, the high cut stress of dislocations through coherent nanoprecipitates, which comes from the chemical ordering effect, accounts for the strengthening behavior. It is also reported that the carbide precipitation hardening in steels can adjust the recrystallization kinetics, realizing YS of ∼1.25 GPa and UTS of ∼1.39 GPa with a uniform elongation of ∼32% and a total elongation of 43% [144]. On the other hand, co-precipitation behavior in steels has been paid much attention. For example, a steel with nanoscale NiAl and Cu precipitates shows UTS of ∼1.9 GPa with a total elongation of ∼10% [145]. Co-precipitation could be a new pathway to design advanced steels [146].

As new promising materials, MEAs and HEAs possess a lot of surprising mechanical and physical properties. However, most HEAs with single-phase FCC structure is not strong enough for practical applications. Thus, nanoprecipitation in HEAs is gradually exploited to obtain desirable mechanical properties. A FeCoNiCr-based HEA is successfully strengthened by coherent nanoscale precipitates, showing a high UTS of ∼1.3 GPa and a good total elongation of 17% [147]. Also, the heterogeneous precipitation behavior in MEA is reported [91]. Precipitation hardening aids the strengthening of MEAs with YS of ∼750 MPa and UTS of ∼1.3 GPa, meanwhile a large plasticity of ∼45% is maintained.

Recently, a new kind of FeCoNi-based alloy achieves high YS of ∼1.0 GPa, UTS of ∼1.5 GPa and a good ductility of ∼50% [148]. Highly alloying with Ti and Al additions leads to the formation of high-density ductile multicomponent intermetallic nanoparticles. Such complex alloy system exhibits an unusual multistage work-hardening behavior, resulting from pronounced dislocation activities (especially high-density dislocation walls) and deformation-induced microbands. With the aid of these microstructures, no strength-ductility trade-off and plastic instability occurs until the tensile strain reaches over 50%. The controllable introduction of multicomponent intermetallic nanoparticles into alloys promotes a new way for advanced structural materials design via nanoprecipitation. Note that the microstructure is similar with "*type 5*" SNDP structure as shown in Fig. 10, except the intrinsic size is larger than 10 nm. Hence, high-density supra-nano precipitation may further improve this kind of advanced materials.

It has long been known that nanoprecipitates in a material are thought to serve as obstacles to dislocation glide and cause hardening of materials. However, this strengthening mechanism is hard to explain the large ductility of high-density nanoprecipitation strengthened materials. The latest achievement by Peng et al. discover that nanoprecipitates can act as a unique type of sustainable dislocation source at sufficiently high stress [149]. Both strength and ductility are enhanced because a dense dispersion of nanoprecipitates simultaneously serve as dislocation sources and obstacles, leading to a sustainable and self-hardening deformation mechanism.

Phase transformation

Phase transformation induced plasticity has been widely utilized in various materials. Some of the high-performance materials mentioned above also thank to the phase transformation mechanism (TRIP effect), which is beneficial for the plasticity and strain hardening. For instance, the plasticity of conventional steels can be increased by TRIP effect, due to the deformation induced austenite to martensite transformation [66,150] and such mechanism also works in HEAs [25]. Besides, the phase boundaries create new obstacles for dislocation movement, which provides strain hardening. Both heat treatment and mechanical processing techniques can tailor these microstructures to optimize the strength-ductility synergy.

Titanium alloy is a representative engineering material which has different allotropic modifications. Alloying, as well as various thermal and mechanical treatments of titanium alloys give rise to the optimization of nanostructures and properties via phase transformation. A kind of low-cost nanostructured β-type titanium alloy with higher strength than all the known commercial counterparts has been successfully manufactured [151]. The phase transformation leads to the formation of hierarchical nanostructures, which could be strength encouraging. Thus, the detailed understanding and control of phase transformation mechanism are important and recently some impressive outcomes can be found [152]. Additionally, the reversible phase transformation behavior is also very important for the practical application of materials [153], one of which is the reversible phase transformation between austenite and martensite [154]. It is essential for the design of shape memory alloys [155,156]. Of course, phase transformation behavior extensively exists in various material systems. The design of high strength and high ductility materials via phase transformation is also one of the state-of-the-art strategies.

Additive manufacturing

Different from the conventional processing pathways based on materials removal methods, additive manufacturing (AM) is based on a discipline of material incremental manufacturing.

With the advancement of AM technology in recent years, the density and quality of AM-produced parts are improved. The density of additively manufactured metals is now comparable to the ones synthesized by conventional process and become applicable in industry. Moreover, the microstructures of materials produced by AM are tunable. Thus, AM gradually becomes a powerful technique to fabricate nanostructural metallic materials.

One of the most popular additively manufactured metallic materials is titanium alloy. A kind of high strength titanium alloy produced by laser metal deposition achieves a fine grain size [157]. Microstructures can be tailored by synergistically engineering the solidification and subsequent eutectoid decomposition behaviors. Manufactured by selective laser melting, β-type titanium alloys exhibit high strength and good ductility because of TRIP and TWIP effects [158,159] and twinning also benefits the fatigue property of titanium alloy [160]. 316L stainless steel can also be produced by AM, showing interesting microstructures and superior mechanical properties. Dislocation networks are observed in the 316L stainless steels fabricated by selective laser melting [161]. The dislocation network can slow down the dislocation motion and promote strong twinning behavior during plastic deformation. During laser powder-bed-fusion manufacturing of 316L stainless steels, the solidification-enabled cellular structures, low-angle GBs and dislocations form, greatly contributing to the enhancement of dislocation pinning and twinning behaviors [23]. Both crystallographic texture and grain size can be tuned in 316L steels produced by selective laser melting [162]. Optimizing crystallographic texture can promote deformation twinning. Recently, high-performance CoCrFeNi high-entropy alloy with nanotwins and precipitates is achieved by 3D ink-extrusion printing [163].

On the other hand, a lot of research work focuses on the exploration of MGs synthesis by AM. For instance, Wu et al. customize an ultrasonic bonding method to manufacture bulk MGs additively from Ni-based MGs strips [164]. The thermal properties almost do not change while the hardness and elastic modulus of such Ni-based MGs are improved compared with the original MGs strips. An Fe-based bulk MG larger than the critical casting thickness is successfully fabricated by selective laser melting, with mechanical properties rivaling that of their cast counterparts [165]. Intriguingly, nano-grain clusters are observed sparsely distributed in the amorphous matrix. It provides a probability to fabricate crystalline/amorphous dual-phase metallic composites. A Zr-based bulk MG produced through laser powder-bed-fusion displays decreased strength while maintaining good wear property compared with casting ones [166]. Besides, another kind of Zr-based MG is built on Ti-6Al-4V substrate by laser foil printing [167]. Its glass transition temperature, crystallization temperature, micro-hardness, and tensile strength are very similar to the conventionally processed counterpart. The printed MG strongly binds with and the Ti substrate. As mentioned above that AM techniques such as magnetic sputtering and pulsed electrodeposition can be employed to synthesize nanostructured MGs. Nevertheless, the available AM techniques for the synthesis of nanostructured MGs are still very limited.

In a word, researchers are capable of tailoring various microstructures in metallic materials by AM. However, precise nanostructure design via AM still has a long way to go. Quantitatively optimizing nanostructures in crystalline materials, introducing nanostructures into MGs and constructing crystalline/amorphous combined materials are all attractive topics for AM of advanced nanostructural metallic materials.

Machine learning

We also would like to appeal the application of machine learning for the design of high-performance nanostructured materials. To date, most scientists are focusing on finding new advanced materials [96,168–170] and predict their diverse properties [171]. By virtue of large materials database, machine learning can envision the key factors for various materials such as the melting temperatures, the formation enthalpy, chemical compositions and band gap energies. Recently, machine learning is being employed to study GBs [97,98]. Since a large amount of data is available owing to the long-time systematic studies on the nanostructures in crystalline materials, machine learning should be very suitable for the advanced materials design via the consideration of the characteristics of nanostructures such as nanotwins, SFs, dislocations and GBs.

Extracting knowledge from huge data by human beings could be incomplete and time-consuming, which can be reconciled by computers. Databases serve as resources for predictive modeling and design. This relies on the development of machine learning methods which enables the establishment of accurate models quickly and automatically. Although great success has been achieved by machine learning, especially for manufacturing new alloys by tuning chemical compositions. Machine learning based development of superb structural metallic materials via nanostructure design is still in its infancy. In particular, a set of attributes that describe the nanostructures in materials for data training and a machine learning algorithm to map structural attributes to properties need to be developed to accelerate the reliable design of high-performance materials.

Conclusions and perspectives

From the perspective of the relationship between specific strength and ductility (Fig. 13), it can be found that most of the high-performance steels contain HNT structures. Notably, the specific strength of high-order HNT pure silver even exceeds that of gradient copper. It should be emphasized that other advanced nanostructures such as gradient structure and dislocation architectures are also utilized with HNT in a material. For the MEAs and HEAs, not only the types and quantities of elements dominate the mechanical properties, appropriate micro-alloying and nanostructure design also play a non-negligible role. Introducing high-density multicomponent intermetallic nanoparticles and ordered oxygen complexes into MEAs and HEAs greatly enhance the mechanical properties. On the other hand, the manipulation of amorphous heterogeneity is a major nanostructuring pathway while far from explored and understood. Nanoglass shows the possibility of fabricating multiphase MGs. Fig. 14 summarizes some superior nanostructures to achieve mechanically high-performance materials with the corresponding processing techniques and strengthening mechanisms.

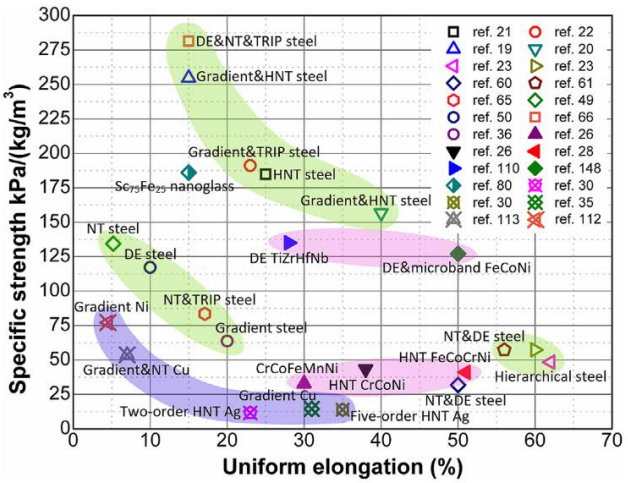

FIGURE 13

A map showing the specific strength and ductility of the advanced nanostructured materials reviewed in this paper (Hollow, solid, half right solid and '×' center scatters represent steels, medium and high entropy alloys, $Sc_{75}Fe_{25}$ nanoglass and pure metals, respectively. "DE" represents "dislocation engineering".).

Appropriate nanostructure design has been demonstrated beneficial to reverse the strength-ductility trade-off. For crystalline materials, the construction of complex NT architecture is a direction worth exploring. More efficient work-hardening capacity could be accessible with the optimization of the intrinsic structural parameters such as the spatial distribution, the twin orders and the combination of HNT thicknesses. Certainly, some other strategies such as (1) tailoring the stability of boundaries or interfaces, (2) optimizing dislocation-based architectures, (3) fabricating gradient nano-grained structure, (4) adjusting the volume fraction, the composition/structure and the diversity of nanoprecipitates, and (5) designing phase transformation based allotropes also need further studies. On the other hand, the structural heterogeneity of MGs gives rise to the strain/stress delocalization, leading to the plasticity of MGs. However, in order to answer the question of how to control the microstructure/heterogeneity (such as the fraction, characteristic size and distribution of free volume) in MGs, the fundamental knowledge of the atomic relaxation behaviors need to be further clarified.

In this review, several types of supra-nano materials are introduced. Each kind of structure contributes to extraordinary mechanical properties, of which, the SNDP-GC with the 'perfect' crystalline and amorphous phases contributes to the near-ideal strength. The good mechanical properties of materials are the basis of device design. For example, the flexible electronic devices or micro-electromechanical systems (MEMS) require materials possessing high strength and deformation capacity. The SNDP-GC film with near-ideal strength and large deformation capacity will be a promising material applied in these areas. Besides, high-

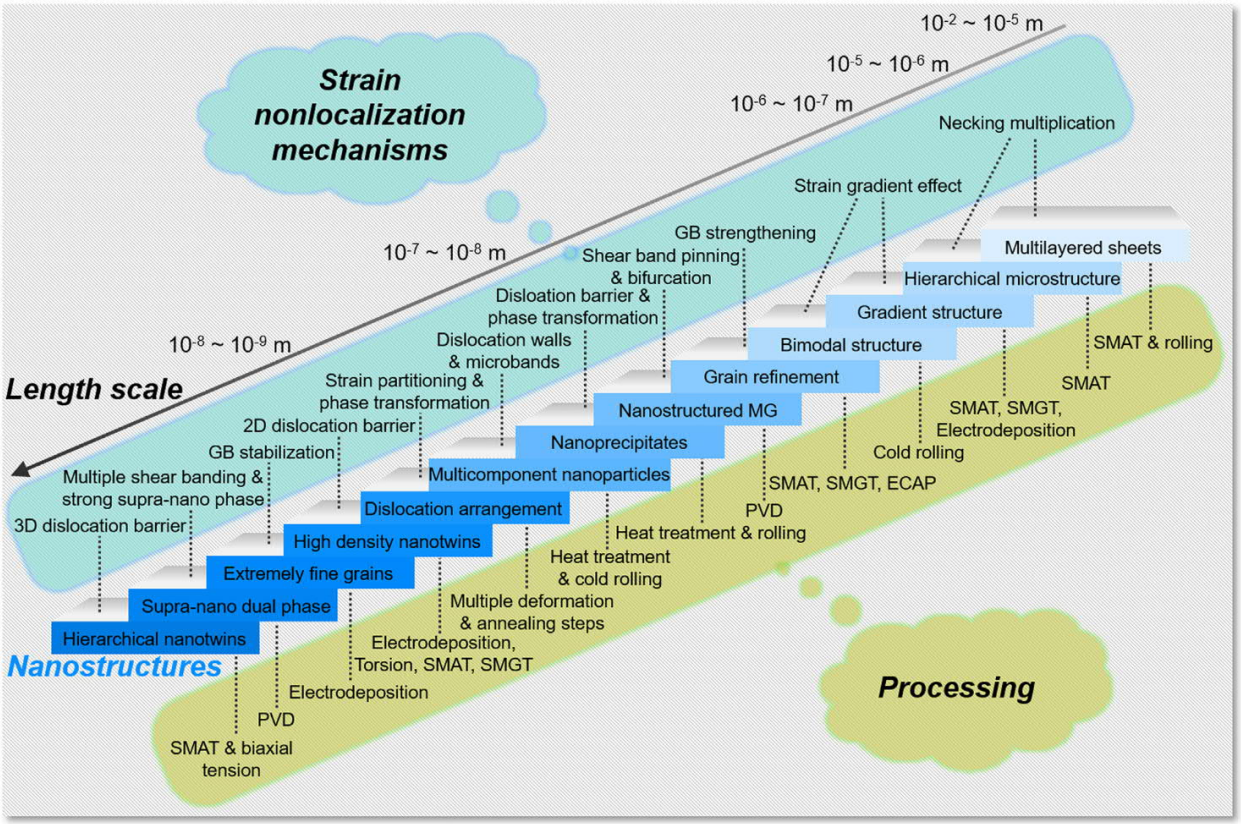

FIGURE 14

An overall flowchart of some representative nanostructures achieving superior mechanical properties with the corresponding processing pathways and strengthening mechanisms.

performance magnetic and catalytic materials usually have crystalline-amorphous composite structure [172–176]. Furthermore, superconducting materials are usually made up with 'perfect' crystalline structure [177,178]. Supra-nanostructuring may provide a way to develop new materials with extraordinary mechanical, magnetic, electronic, superconductive or catalytic properties.

The thermal and mechanical instability of GBs in polycrystalline metals induces grain growth, rotation or migration that undermine the mechanical properties. These phenomena may be eliminated in the SNDP-GC structure. Because the heterogeneous interface between supra-nano crystals and MGs may form particular short-range order structures that different from the interior region of MGs [179]. Such unique topological structure at interface subsequently improves the thermal and mechanical stability of SNDP-GC structure, such as impeding grain growth/rotation and crystallization of MGs [180]. Thus, the advanced SNDP-GC nanostructure design may break through the application bottleneck of conventional nanostructured metal materials. Nevertheless, what needs to be pointed out is that the studies on this new class of structural nanomaterials is still staying at a very preliminary stage and some important issues can be proposed, such as designing stable heterogeneous interfaces and understanding the deformation mechanisms of different supra-nano materials, coupled with intrinsic size effects and plasticity of amorphous phase.

All the progresses made in the research area of structural metallic materials, as reviewed in this paper, can be classified as chemical, physical and topological heterogeneity (Fig. 15). Heterogeneity engineering can effectively improve mechanical properties of metals by enhancing the behavior of strain delocalization [181]. Recently, the universal chemical heterogeneity of the HEAs is unraveled [182]. The researchers reveal a pronounced chemical heterogeneity, leading to an increase of SFE and thus, significantly enhances the dislocation induced physical heterogeneity and obtain outstanding mechanical properties. On the other hand, manipulating the short and medium range order of atoms in MGs varies their deformation behavior and improves ductility. Beyond topological heterogeneity, chemical heterogeneity increases the difficulty for cavitation initiation, leading to a high toughness [183]. Besides, through room temperature cyclic deformation, physical heterogeneity can be introduced into aluminum alloys by injecting vacancies [184], consequently mediating solute precipitation and enhance strength and elongation. Glass-crystal dual-phase composite materials usually have chemical heterogeneity [42]. In addition, topological heterogeneity also exists, especially at the interfaces between two phases. By tuning the heterogeneities at nanoscale, unprecedently strong magnesium alloy [71] and advanced aluminum alloy with high strength and high ductility are successfully developed [185]. The nanocrystal-glass interface in this advanced aluminum alloy facilitates ultrahigh strength by impeding dislocation propagation among nanograins and the flow behavior of the nano-sized MG phase results in increased plasticity.

The understanding of the relationship of structure–property-mechanism for materials has been further deepened. Still some key points of particular interest for future research are outlined:

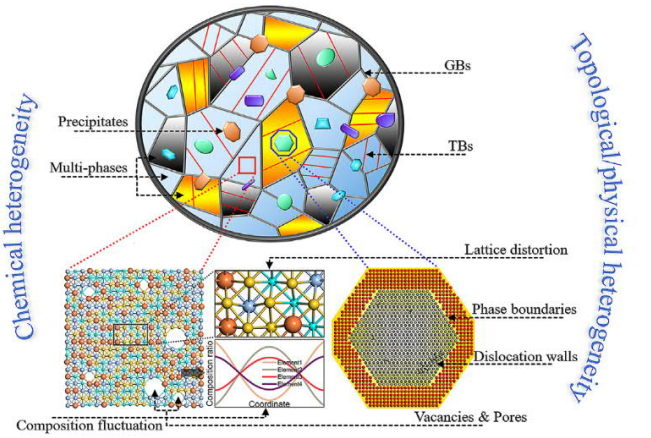

FIGURE 15

A schematic diagram showing some representatives of chemical, physical and topological heterogeneity in metallic materials.

1. Beyond exploring the relationship of structure–property-mechanism, systematically constructing the relation between structural characteristics and fabrication conditions is essential to realize controllable adjustment of mechanical properties via the precise regulation of nanostructures.
2. The formation mechanisms of various nanostructures either by top-down or bottom-up approaches, should be firmly clarified to establish general nanostructure preparation theories. A series of key parameters are expected to be found and used to determine/tailor the formation ability of nanostructures, accelerating the development of high-performance nanostructural metallic materials.
3. Experimental characterization, computer simulations and theoretical modeling of the strength and ductility enhancement mechanisms still need further exploration, especially for the newly developed nanostructures such as HNTs, nanostructured MGs, supra-nanostructures.
4. Many advanced processing techniques can introduce various nanostructures into one material. The comprehensive understanding of the interplay of these nanostructures may aid the development of multi-structure optimization strategies, further optimizing the mechanical properties of materials.
5. With the knowledge of the relationship of fabrication-structure–property-mechanism, it is essential to advance the existing techniques and develop new manufacturing technology particularly aiming to meet the needs of industrial manufacturing.

In a word, the synthesis of advanced structures is an effective way to produce high-strength and high-ductility materials. In particular, developing modern techniques to introduce multiple advanced nanostructures into one material could further improve the overall mechanical properties. Furthermore, it is just the beginning of the era of supra-nano materials [186]. We firmly believe that the supra-nano dual-phase or even multi-phase systems can further enrich the nanostructure design approaches, such as simultaneously taking advantage of the intelligent design of crystalline/glassy phases and utilizing the potential synergies

between them, especially through a rational coupling of chemical distribution, physical structures and topological configurations. Many other materials in this new material family will be developed in the near future.

Declaration of Competing Interest

The authors declare that they have no known competing financial interests or personal relationships that could have appeared to influence the work reported in this paper.

Acknowledgements

J.L. gratefully acknowledges the supports of the National Key R&D Program of China (Project No. 2017YFA0204403), the Major Program of the National Natural Science Foundation of China (NSFC) grant 51590892, the Hong Kong Collaborative Research Fund (CRF) Scheme (C4026-17W), Theme-based Research Scheme (Ref. T13-402/17-N) and General Research Fund (GRF) Scheme (CityU 11247516, CityU 11209918, CityU 11216219). Q.W. would like to thank the supports of NSFC grant 51871140 and NSFS (No. 18ZR1414700).

References

[1] L. Lu et al., Science 304 (2004) 422–426.
[2] L. Lu et al., Science 323 (2009) 607–610.
[3] Y. Tian et al., Nature 493 (2013) 385–388.
[4] Q. Huang et al., Nature 510 (2014) 250–253.
[5] L. Sun et al., Carbon 127 (2018) 320–328.
[6] X. Li et al., Nature 464 (2010) 877–880.
[7] L. Zhu et al., Acta Mater. 59 (2011) 5544–5557.
[8] L.G. Sun et al., Mater. Sci. Eng. A-Struct. Mater. Prop. Microstruct. Process. 606 (2014) 334–345.
[9] D. Jang et al., Nat. Nanotechnol. 7 (2012) 594–601.
[10] Z. You et al., Acta Mater. 61 (2013) 217–227.
[11] L.G. Sun et al., Philos. Mag. 95 (2015) 3467–3485.
[12] S. Qu et al., Acta Mater. 57 (2009) 1586–1601.
[13] P. Mullner, A.H. King, Acta Mater. 58 (2010) 5242–5261.
[14] D.Y. Cong et al., Acta Mater. 59 (2011) 7070–7081.
[15] L.L. Zhu et al., Appl. Phys. Lett. 101 (2012) 081906.
[16] L.L. Zhu et al., J. Mech. Phys. Solids 76 (2015) 162–179.
[17] F.P. Yuan, X.L. Wu, J. Appl. Phys. 113 (2013) 203516.
[18] L.G. Sun et al., Philos. Mag. 94 (2014) 4037–4052.
[19] H.N. Kou et al., Adv. Mater. 26 (31) (2014) 5518–5524.
[20] Y.J. Wei et al., Nat. Commun. 5 (2014) 3580.
[21] P. Zhou et al., Acta Mater. 111 (2016) 96–107.
[22] X.L. Wu et al., Acta Mater. 112 (2016) 337–346.
[23] Y.M. Wang et al., Nat. Mater. 17 (2018) 63–71.
[24] C.W. Shao et al., Acta Mater. 145 (2018) 413–428.
[25] Z.M. Li et al., Nature 534 (2016) 227–230.
[26] G. Laplanche et al., Acta Mater. 128 (2017) 292–303.
[27] Z.J. Zhang et al., Nat. Commun. 8 (2017) 14390.
[28] B. Cai et al., Acta Mater. 127 (2017) 471–480.
[29] A.Y. Chen et al., Nat. Commun. 10 (2019) 1403.
[30] X. Liu et al., Acta Mater. 149 (2018) 397–406.
[31] L.G. Sun et al., Int. J. Plast. 128 (2020), https://doi.org/10.1016/j.ijplas.2020.102685 102685.
[32] J. Li, K.G. Wang, J. Mater. Res. (2019) 2177–2193.
[33] E. Ma, T. Zhu, Mater. Today 20 (2017) 323–331.
[34] L.G. Sun et al., npj Comput. Mater. 4 (2018) 6.
[35] T.H. Fang et al., Science 331 (2011) 1587–1590.
[36] X.L. Wu et al., Proc. Natl. Acad. Sci. U. S. A. 111 (2014) 7197–7201.
[37] J.J. Li et al., Int. J. Plast. 88 (2017) 89–107.
[38] K. Lu, Science 345 (2014) 1455–1456.
[39] T.J. Rupert et al., J. Mater. Res. 27 (2012) 1285–1294.
[40] B. Chen et al., Science 338 (2012) 1448–1451.
[41] X.C. Liu et al., Science 342 (2013) 337–340.
[42] Z.Y. Yu et al., Science 358 (2017) 97–101.
[43] K. Lu, Nat. Rev. Mater. 1 (2016) 16019.
[44] X.Y. Li, K. Lu, Nat. Mater. 16 (2017) 700–701.
[45] J. Hu et al., Science 355 (2017) 1292–1296.
[46] G.I. Taylor, Proc. R. Soc. Lond. Ser. A 145 (1934) 362–387.
[47] X.D. Zhang et al., Acta Mater. 59 (2011) 3422–3430.
[48] P.V. Liddicoat et al., Nat. Commun. 1 (2010) 63.
[49] F.K. Yan et al., Scr. Mater. 84–85 (2014) 31–34.
[50] A. Vinogradov et al., Acta Mater. 106 (2016) 295–303.
[51] K.A. Nibur et al., Acta Mater. 54 (2006) 2677–2684.
[52] S. Wang et al., Acta Mater. 135 (2017) 96–102.
[53] J. Takahashi et al., Acta Mater. 107 (2016) 415–422.
[54] A. Kwiatkowski da Silva et al., Acta Mater. 147 (2018) 165–175.
[55] H. Pan et al., Acta Mater. 149 (2018) 350–363.
[56] D. Akama et al., ISIJ Int. 56 (2016) 1675–1680.
[57] M.D. McMurtrey et al., Int. J. Plast. 56 (2014) 219–231.
[58] M.J. Lai et al., Acta Mater. 100 (2015) 290–300.
[59] D. Canadinc et al., Mater. Sci. Eng. A-Struct. Mater. Prop. Microstruct. Process. 454 (2007) 662–666.
[60] I. Gutierrez-Urrutia, D. Raabe, Acta Mater. 59 (2011) 6449–6462.
[61] I. Gutierrez-Urrutia, D. Raabe, Acta Mater. 60 (2012) 5791–5802.
[62] S. Morito et al., Acta Mater. 54 (2006) 5323–5331.
[63] S. Chatterjee et al., Mater. Sci. Technol. 22 (2006) 641–644.
[64] B.B. He et al., J. Mater. Sci. Technol. 33 (2017) 1494–1503.
[65] M.M. Wang et al., Acta Mater. 85 (2015) 216–228.
[66] B.B. He et al., Science 357 (2017) 1029–1032.
[67] H. Gleiter, Nanotruct. Mater. 6 (1995) 3–14.
[68] M.F. Ashby, A.L. Greer, Scr. Mater. 54 (2006) 321–326.
[69] C. Schuh et al., Acta Mater. 55 (2007) 4067–4109.
[70] M.M. Trexler, N.N. Thadhani, Prog. Mater. Sci. 55 (2010) 759–839.
[71] G. Wu et al., Nature 545 (2017) 80–83.
[72] H. Gleiter et al., Nano Today 9 (2014) 17–68.
[73] H. Gleiter, Small 12 (2016) 2225–2233.
[74] N. Chen et al., J. Alloys Compd. 707 (2017) 371–378.
[75] J. Eckert et al., J. Mater. Res. 22 (2011) 285–301.
[76] H. Gleiter, Acta Mater. 56 (2008) 5875–5893.
[77] J.X. Fang et al., Nano Lett. 12 (2012) 458–463.
[78] I. Singh et al., Philos. Mag. Lett. 94 (2014) 678–687.
[79] X.L. Wang et al., Scr. Mater. 98 (2015) 40–43.
[80] K. Albe et al., Mech. Mater. 67 (2013) 94–103.
[81] R. Witte et al., Appl. Phys. Lett. 103 (2013) 073106.
[82] N. Chen et al., J. Mater. Chem. B 1 (2013) 2568.
[83] S.V. Ketov et al., Sci. Rep. 5 (2015) 7799.
[84] G. Richter et al., Nano Lett. 9 (2009) 3048–3052.
[85] C. Deng, F. Sansoz, ACS Nano 3 (2009) 3001–3008.
[86] L. Tian et al., Nat. Commun. 3 (2012) 609.
[87] L. Lu et al., Science 287 (2000) 1463–1466.
[88] J. Schiøtz, K.W. Jacobsen, Science 301 (2003) 1357–1359.
[89] R. Babilas et al., J. Non-Cryst. Solids 505 (2019) 421–430.
[90] S.H. Jiang et al., Nature 544 (2017) 460–464.
[91] Y.L. Zhao et al., Acta Mater. 138 (2017) 72–82.
[92] D. Herzog et al., Acta Mater. 117 (2016) 371–392.
[93] D.D. Gu et al., Int. Mater. Rev. 57 (2012) 133–164.
[94] J.J. Lewandowski, M. Seifi, Annu. Rev. Mater. Res. 46 (2016) 151–186.
[95] P.C. Collins et al., Annu. Rev. Mater. Res. 46 (2016) 63–91.
[96] G. Hautier et al., Chem. Mat. 22 (2010) 3762–3767.
[97] C.W. Rosenbrock et al., npj Comput. Mater. 3 (2017) 29.
[98] J.A. Gomberg et al., Acta Mater. 133 (2017) 100–108.
[99] F. Zhang et al., Eng. Fract. Mech. 201 (2018) 29–35.
[100] J.J. Li et al., Mater. Res. Lett. 3 (2015) 190–196.
[101] Y. Liu, J. Zhou, Eng. Fract. Mech. 204 (2018) 63–71.
[102] X.C. Liu et al., Acta Mater. 96 (2015) 24–36.
[103] D.A. Hughes, N. Hansen, Phys. Rev. Lett. 112 (2014) 135504.
[104] X.L. Zhou et al., Phys. Rev. Lett. 118 (2017) 096101.
[105] Z. Huang et al., Acta Mater. 148 (2018) 110–122.
[106] Q. Li et al., Adv. Mater. 30 (2018) 1704629.
[107] X. Zhou et al., Nature 579 (2020) 67–72.
[108] M. Kuzmina et al., Science 349 (2015) 1080–1083.
[109] G.J. Cheng et al., Acta Mater. 148 (2018) 344–354.
[110] Z. Lei et al., Nature 563 (2018) 546–550.
[111] H. Yu et al., Mater. Sci. Eng. A-Struct. Mater. Prop. Microstruct. Process. 710 (2018) 10–16.
[112] R. Cao et al., Mater. Today 32 (2020) 94–107.
[113] Z. Cheng et al., Science 362 (2018) eaau1925.
[114] I.A. Ovid'ko et al., Prog. Mater. Sci. 94 (2018) 462–540.

[115] J. Li, A.K. Soh, Int. J. Plast. 39 (2012) 88–102.
[116] J. Li et al., Mater. Sci. Eng. A-Struct. Mater. Prop. Microstruct. Process. 620 (2015) 16–21.
[117] X. Lu et al., Int. J. Plast. 113 (2019) 52–73.
[118] J. Zhao et al., Int. J. Plast. 125 (2020) 314–330.
[119] L.L. Zhu et al., Acta Mater. 128 (2017) 375–390.
[120] K. Wu et al., Mater. Sci. Eng. A-Struct. Mater. Prop. Microstruct. Process. 703 (2017) 180–186.
[121] L.L. Zhu et al., Scr. Mater. 133 (2017) 49–53.
[122] L.L. Zhu et al., Int. J. Plast. 114 (2019) 272–288.
[123] N. Chen et al., Nanotechnology 24 (2013) 045610.
[124] M. Ghafari et al., Appl. Phys. Lett. 100 (2012) 133111.
[125] X. Wang et al., Scr. Mater. 116 (2016) 95–99.
[126] J.R. Greer, J.T.M. De Hosson, Prog. Mater. Sci. 56 (2011) 654–724.
[127] S. Wang et al., J. Mech. Phys. Solids 77 (2015) 70–85.
[128] S. Wang et al., J. Appl. Phys. 119 (2016) 245113.
[129] A.L. Greer et al., Mater. Sci. Eng. R-Rep. 74 (2013) 71–132.
[130] D.Z. Chen et al., Nano Lett. 13 (2013) 4462–4468.
[131] M.Q. Jiang, L.H. Dai, J. Mech. Phys. Solids 57 (2009) 1267–1292.
[132] P. Thamburaja, J. Mech. Phys. Solids 59 (2011) 1552–1575.
[133] S.S. Hirmukhe et al., Comput. Mater. Sci. 161 (2019) 83–92.
[134] D. Jang, J.R. Greer, Nat. Mater. 9 (2010) 215–219.
[135] S.H. Nandam et al., Acta Mater. 136 (2017) 181–189.
[136] A. Chen et al., Acta Mater. 59 (2011) 3697–3709.
[137] L.Y. Chen et al., Nature 528 (2015) 539–543.
[138] S.H. Kim et al., Nature 518 (2015) 77–79.
[139] W. Rao et al., Mech. Mater. 103 (2016) 68–77.
[140] J.C. Li et al., J. Alloys Compd. 737 (2018) 271–294.
[141] Y. Jiang, J. Non-Cryst, Solids 484 (2018) 118–123.
[142] M. Pu et al., Mater. Sci. Eng. A-Struct. Mater. Prop. Microstruct. Process. 734 (2018) 129–138.
[143] D. Raabe et al., Scr. Mater. 60 (2009) 1141–1144.
[144] J.L. Zhang et al., Acta Mater. 141 (2017) 374–387.
[145] Z.B. Jiao et al., Acta Mater. 97 (2015) 58–67.
[146] Z.B. Jiao et al., Mater. Today 20 (2017) 142–154.
[147] J.Y. He et al., Acta Mater. 102 (2016) 187–196.
[148] T. Yang et al., Science 362 (2018) 933–937.
[149] S. Peng et al., Proc. Natl. Acad. Sci. U. S. A. 117 (2020) 5204–5209.
[150] P.J. Jacques, Curr. Opin. Solid State Mat. Sci. 8 (2004) 259–265.
[151] A. Devaraj et al., Nat. Commun. 7 (2016) 11176.
[152] A.R. Kilmametov et al., Acta Mater. 144 (2018) 337–351.
[153] Y.T. Song et al., Nature 502 (2013) 85–88.
[154] X. Chen et al., J. Mech. Phys. Solids 61 (2013) 2566–2587.
[155] J. Cui et al., Nat. Mater. 5 (2006) 286–290.
[156] R. Zarnetta et al., Adv. Funct. Mater. 20 (2010) 1917–1923.
[157] D.Y. Zhang et al., Nature 576 (2019) 91–95.
[158] Y.J. Liu et al., Materialia 6 (2019) 100299.
[159] N. Hafeez et al., J. Alloys Compd. 790 (2019) 117–126.
[160] Y.J. Liu et al., Addit. Manuf. 32 (2020) 101060.
[161] L.F. Liu et al., Mater. Today 21 (2018) 354–361.
[162] Z.J. Sun et al., NPG Asia Mater. 10 (2018) 127–136.
[163] C. Kenel et al., Nat. Commun. 10 (2019) 904.
[164] W.Z. Wu et al., J. Non-Cryst. Solids 506 (2019) 1–5.
[165] Z. Mahbooba et al., Appl. Mater. Today 11 (2018) 264–269.
[166] P. Bordeenithikasem et al., Addit. Manuf. 21 (2018) 312–317.
[167] Y.Q. Li et al., Acta Mater. 144 (2018) 810–821.
[168] P. Raccuglia et al., Nature 533 (2016) 73–76.
[169] A.O. Oliynyk, A. Mar, Accounts Chem. Res. 51 (2018) 59–68.
[170] A.R. Natarajan, A. Van der Ven, npj Comput. Mater. 4 (2018) 56.
[171] L. Ward et al., npj Comput. Mater. 2 (2016) 16028.
[172] J. Gao et al., Appl. Phys. Lett. 99 (2011) 052504.
[173] Z. Jia et al., Adv. Funct. Mater. 27 (2017) 1702258.
[174] S.X. Liang et al., Adv. Mater. 30 (2018) 1802764.
[175] L.C. Zhang et al., Prog. Mater. Sci. 105 (2019) 100576.
[176] Z. Jia et al., Adv. Funct. Mater. 29 (2019) 1807857.
[177] Y. Hidaka, M. Suzuki, Nature 338 (1989) 635–637.
[178] C.L. Song et al., Science 332 (2011) 1410–1413.
[179] Z.L. Pan, T.J. Rupert, Comput. Mater. Sci. 131 (2017) 62–68.
[180] Q. Wang et al., Phys. Rev. Lett. 106 (2011) 215505.
[181] A.Y. Chen et al., Scr. Mater. 59 (2008) 579–582.
[182] Q. Ding et al., Nature 574 (2019) 223–227.
[183] Q. An et al., Proc. Natl. Acad. Sci. U. S. A. 113 (2016) 7053–7058.
[184] W. Sun et al., Science 363 (2019) 972–975.
[185] G. Wu et al., Nat. Commun. 10 (2019) 5099.
[186] J. Zhang et al., Mater. Today 37 (2020) 18–26, https://doi.org/10.1016/j.mattod.2020.02.020.